Characterization of VOCs and their related atmospheric processes in a central China city during severe ozone pollution periods

Bowei Li[1], Steven Sai Hang Ho[2,3*], Sunling Gong[1,4*], Jingwei Ni[1], Huairui Li[1], Liyan Han[1], Yi Yang[1], Yijin Qi[1], Dongxu Zhao[1]

[1] *Langfang Academy of Eco Industrialization for Wisedom Environment, Langfang 065000, China*

[2] *Division of Atmospheric Sciences, Desert Research Institute, Reno, Nevada, USA*

[3] *Key Lab of Aerosol Chemistry & Physics, Institute of Earth Environment, Chinese Academy of Sciences, Xi'an 710061, China*

[4] *Center for Atmosphere Watch and Services of CMA, Chinese Academy of Meteorological Sciences, Beijing 100081, China*

*Correspondence to: Steven Sai Hang Ho (stevenho@hkpsrl.org) and Sunling Gong (gongsl@cma.gov.cn)

Revision on: October 27, 2018

Abstract

A five-month campaign (from May to September 2017) was conducted to characterize volatile organic compounds (VOCs) for the first time at four sites in Zhengzhou City, Henan Province, China, where ozone (O_3) concentration shown an increasing trend in recent years. Canister samples were collected for measurement of fifty-seven VOCs, which are the most important O_3 precursors. During the same period, O_3 and its precursor gases were monitored online simultaneously. The results indicated that the average mixing ratio of total quantified VOCs (Σ_{VOCs} = 28.83±22.05 ppbv) in Zhengzhou was lower than that in the other Chinese megacities, while alkyne was a higher proportion. The abundances, compositions and ratios of typical VOCs showed clear spatial and temporal variations. The cluster analysis that air masses from south of Zhengzhou were cleaner than from other directions. the molar ratio of VOCs to NO_x indicated that VOCs than NO_x in Zhengzhou. The source apportionment was conducted with Positive Matrix Factorization (PMF), and it was found that vehicle exhaust, coal and biomass burning, and solvent usage were the major sources for ambient VOCs at all four sites. From Potential Source Contribution Function (PSCF) analysis, the strong emissions from coal+biomass burning and solvent usage were concentrated in southwest of Shanxi and Henan province. The results of this study gather scientific evidences on the pollution sources for Zhengzhou city, benefiting the Government to establish efficient environmental control measures particularly for O_3 pollution.

1. Introduction

Volatile organic compounds (VOCs) are diverse and reactive chemicals. Vehicle exhausts, fuel combustion and evaporation, and solvent usage are the known major anthropogenic sources of VOCs (Zhang et al., 2014;Liu et al., 2017;Sahu et al., 2017). VOCs play a crucial role in the ground-level ozone (O_3) pollution which has troubled many rapid economy-growth urban cities

(Wang et al., 2017b;Nagashima et al., 2017). Many related studies are thus being conducted globally (Wei et al., 2014;Malley et al., 2015;Ou et al., 2015). In China, the investigations on VOCs including source apportionment, measurement of emission profiles and interpretation of seasonal variations were mainly concentrated in Yangtze River Delta (YRD), Pearl River Delta (PRD) and Beijing-Tianjin (BJT) regions (An et al., 2014;Wang et al., 2014;Chen et al., 2014;Liu et al., 2016;Guo et al., 2017). Limited studies have been conducted in less developed or developing regions (i.e., southwestern and northwestern China) where prominently impacted by biomass burning and with high abundances of toxic and reactive compounds (Li et al., 2014;Li et al., 2017a).

Fifty-seven VOCs, including C_2 - C_{10} alkanes, alkenes, alkynes and aromatics, which greatly contribute to ambient O_3 formation, have been identified and are regularly monitored by Photochemical Assessment Monitoring Stations (PAMS) (Zhao et al., 2016;Chen et al., 2010). Due to characteristic structure and reactivity of these compounds, their contributions in O_3 production were varied accordingly, and it is reported that aromatics and alkenes were responsible for most of the weighted reactivity of VOCs (59.4% and 25.8%, respectively) in Pearl River Delta (PRD) region in China (Ou et al., 2015). Consequently, researchers have deduced that reductions of alkenes and aromatics are profit for O_3 control (Carter 1994). In addition, with the variations on energy structure, industrial construction and meteorological conditions (Wang et al., 2015;Shao et al., 2011), major emission sources of VOCs at each city are unique. In less developed cities of Heilongjiang and Anhui, biomass combustion had the highest contribution (40% and 36%, respectively) to the O_3 formation potentials due to high quantity of agricultural activities, while in the developed cities such as Shanghai, Beijing and Zhejiang, solvent usage has become more dominant (>20%) than other pollution sources (Wu and Xie, 2017). Therefore, identification on district emission sources of VOCs is necessary to provide scientific-based information for policy-makers who establish efficient strategies to alleviate O_3 pollution.

In addition to the factors discussed above, non-linear relationships between ambient VOCs, nitrogen oxide (NO_x) and O_3 production indicate that the reduction in tropospheric O_3 is more complex than expected (Lin et al., 1998;Hidy and Blanchard, 2015;Li et al., 2018). Many modeling

and field studies showed that photochemical O_3 production in several cities in China such as Guangzhou, Shanghai and Beijing with high levels of NO_x were highly sensitive to VOCs (Shao et al., 2009;Gao et al., 2017;Ou et al., 2016). The sensitivity regime is always varied with time and geographical locations (Luecken et al., 2018). The percentage of VOC-limited regime in North China Plain (NCP) increased from 4% to 6% between 2005-2013, owing to the rapid increases of NO_x emissions (Jin and Holloway, 2015).

Zhengzhou City is an important developing city in the mid-west of the Huanghe-Huaihe river flood plain in China. As the capital city of Henan Province, it is densely populated with more than seven million residents in 2010 (Geng et al., 2013). With the rapid growth of industrial activities, as well as increased vehicle emissions and fuel combustions, air quality in Zhengzhou has ~~notoriously~~ deteriorated. The Air quality index (AQI) for 65% of the days in 2013 exceeded the allowable limits of 100 established by the Air Quality Guidel Particularly~~,~~ O_3 was the major pollutant in summer and over 50% of the days in a year, the mixing ratio of O_3 exceeded the Grade I standard (100 µg m^{-3}) of daily maximum average 8-hour (DMA8) in Henan (Shen et al., 2017;Gong et al., 2017). As one of the major precursors of O_3, the study on VOCs is of significance for Zhengzhou, since no related researches are published in peer-reviewed literature. In this work, a comprehensive sampling campaign for VOCs measurement and characterization has been conducted at four monitoring stations during the time period of May - September 2017. The spatial and temporal variations in VOCs in Zhengzhou were determined. The contributions of major emission sources were quantified, and the relationship among O_3-VOCs-NO_x was discussed in details. The results and implications from this study can provide useful guidance for policy-makers to alleviate ozone pollution in Zhengzhou, China.

2. Observation and Methodology

2.1 Sampling site

Based on the density of population distribution, locations of industrial facilities, and the prevailing winds, four sites have been selected for sample collection: Jingkai community (JK; 113.73°E, 34.72°N), municipal environmental monitoring station (MEM; 113.61°E, 34.75°N),

Yinhang school (YH; 113.68°E, 34.80°N) and Gongshui company (GS; 113.57°E, 34.81°N), which are located at the southeastern, southwestern, northeastern and northwestern of Zhengzhou, respectively (Fig. 1). There is a main airport highway and heavy-traffic ring roads approximately 500 m west of JK. Furthermore, the site is at a distance of 2 km from an industrial area, which involves packaging and printing plants, and material distribution factories. It is noteworthy that there are three coal-fired power plants in the urban area of Zhengzhou city. One of the power plants with the highest production was 1.6 km northwest of MEM. Both the MEM and YH include a mix of commercial and condensed residential areas, whereas the apartments around YH are more aged. The GS site is surrounded by several manufacturing plants, including pharmaceuticals, materials, foods and machineries.

Ten sampling days with the rainfall record ($ca.$ 6 mm) were chosen in every month during the period of May - September, 2017 consequently, to represent a typical air quality condition in a month. Grab samples were collected minute using 3.2 L stainless-steel canisters (Entech Instrument, Inc., Simi Valley, CA, USA), which were pre-cleaned with high purity nitrogen and pressurized to 20 psi. Two samples, one collected at 07:00 with increasing of human activities and another one collected at 14:00 with well-mixed of ambient air, were obtained on each sampling day. There was a total of 400 samples collected in this study. The chemical analysis was accomplished within two weeks after the collection of samples. Real-time data for trace gases, including SO_2, CO, NO_2 and O_3, and synchronous meteorological data, such as temperature (T), relative humidity (RH), wind direction (WD) and wind speed (WS), were recorded at each air monitoring station.

2.2 Chemical Analysis

In this study, the measurement of VOCs was based on Compendium Method TO-15, which was established by U.S. EPA. Air in the canister was concentrated using liquid-nitrogen at -160 °C in a cryogenic pre-concentrator (7100A, Entech Instrument, Inc.). Both the CO_2 and H_2O were removed from the transfer line. The air was then thermally desorbed at 120 °C and transferred for analysis to a gas chromatography (GC, 7890A, Agilent Technologies, Santa Clara, CA, USA) coupled with dual detectors, i.e. a mass spectrometric detector (MSD) and a flame ionization detector (FID) (5977E, Agilent Technology). Dual columns were applied for the simultaneous

124 analysis of C_2 - C_{11} hydrocarbons. A PLOT column (15 m, internal diameter of 0.32 mm and film

125 thickness of 3.0 μm) was connected to the FID for detection of C_2 - C_5 NMHCs, whereas C_5 - C_{10}

126 NMHCs, oxygenated VOCs (OVOCs) and halocarbons were separated using a DB-624 column (30

127 m×0.25 mm inner diameter × 3.0 μm film thickness), which was connected to the MSD. Target

128 compounds were identified with retention time and mass spectra, and quantified with multi-point

129 calibration curve in this study. The standard gas of PAMS (1 ppm; Spectra Gases Inc, NJ, USA)

130 was used to construct the calibration curves for the 57 target VOCs, including 28 alkanes, 11

131 alkenes, acetylene and 17 aromatics. Detailed information on the target analyses involved in this

132 study and their corresponding linearity of calibration (R^2), measurement relative standard deviation

133 (RSD), method detection limit (MDL), maximum increment reactivity (MIR, earter, 2010) are

134 presented in Table S1.

135 2.3 Positive matrix factorization (PMF)

136   The U.S. EPA PMF 5.0 software was used for source apportionment (Lau et al., 2010;Abeleira

137 et al., 2017;Xue et al., 2017). Due to the complex chemical reactions, the application of PMF in

138 VOCs has to be based on a couple of principles: eliminating species with mixing ratios below MDL

139 and excluding species with high reactivity, except for the source markers (Shao et al., 2016;Guo et

140 al., 2011). Finally, 31 VOC species and NO_2 were chosen for the source apportionment analysis.

141   In this study, PMF was performed with fifty base runs for each site, results with the minimum

142 Q value (a parameter used to express uncertainties of PMF results) were considered as optimum

143 solutions. In Table S2 the r^2 between observed values and predicted values of selected VOCs and

144 NO_2 are presented for the four sites, the r^2 for most species (>80%) were higher than 0.6,

145 compounds with $r^2<0.6$ were down weighted when determine factor sources.

146   During PMF analysis, bootstrap method was used to evaluate stability and uncertainty of the

147 base run solution, setting the minimum correlation R-value at 0.6, 100 bootstrap runs were

148 performed, and the results were showing in Table S3, and acceptable results (>80%) were gained

149 for all the factors.

150   Three to nine factors were selected to initiate the running of PMF, the Q/Q(exp) for every site

151   at fixed factor size were presented in Table S4. With the increase of factor number, the ratios

152   Q/Q(exp) were declined due to additional factors. When the factor size changing from 3 to 4, 4 to 5,

153   and 5 to 6, the decrement of Q/Q(exp) were larger (~18-25%), while the change was lower than 12%

154   after factors increased to 7, combined with the field conditions, six factors were defined at each

155   site.

156   **2.4 Potential source contribution function (PSCF)**

157   In this study, the probability of air clusters with source concentration higher than a certain

158   value was estimated (Hopke et al., 1995). Briefly, the PSCF value in ij^{th} grid was the ratio of the

159   number of endpoints with higher source concentration relative to the total number of endpoints in

160   ij^{th} grid cell. The criterion value, equal to 75th percentile of the targeted source concentration in this

161   study, was used to verdict whether the value was higher or not. The 48-hour back trajectories was

162   calculated with Hybrid Single-Particle Lagrangian Integrated Trajectory (HYSPLIT) model. ~~While~~

163   there are many grid cells with small values, which could result in high uncertainty, ~~the weight~~

164   function (Wij) was introduced ~~to gain optimized PSCF results~~ (WPSCF) (Polissar et al., 1999).

165   According to average values of end points in each cell, in this case, Wij was presented as below.

$$
Wij = \begin{cases} 1.0 & nij > 30 \\ 0.7 & 10 < nij \leq 30 \\ 0.42 & 5 < nij \leq 10 \\ 0.05 & nij \leq 5 \end{cases}
$$

166

167   **2.5 Estimation of the initial NO_x and VOCs**

168   With the assumption that chemical loss of NO_x and VOCs were mainly due to their reactions

169   with hydroxyl radical (•OH), the initial mixing ratio of NO_x can be calculated with the equation as

170   (Shiu et al., 2007;Shao et al., 2009):

171    $[NO_x]=[NO_x]_0 \exp (-k [•OH] \Delta t)$ (1)

where k stands for the reaction rate between NO_x and [•OH]. In this study, k was set as the observed average ratio of NO_2/NO_x during this campaign.

The photochemical age Δt ~~was usually displayed as~~ the ratio between ~~the~~ two compounds, ~~which~~ emitted from common source, but ~~owning~~ different reaction rate with •OH. For this case, the photochemical age clock was performed with ethylbenzene (E) and m,p-xylene (X) (Sun et al., 2016).

$$[•OH] \quad \Delta t=1/(k_x-k_E) [\ln(C_X/C_E)-\ln(X_0/E_0)] \qquad (2)$$

which k_x and k_E represent their rate constants with •OH, C_X and C_E correspond to the observed mixing ratios; X_0 and E_0 were their initial concentrations. The X_0/E_0 was ~~prescribed at 5~~ percentile of the observed ratios at 07:00 in this paper.

The initial mixing ratio of VOC was estimated with the method as NO_x (Shiu et al., 2007):

$$[VOC]_0=[VOC]_t \exp (k_i [•OH] \Delta t) \qquad (3)$$

where $[VOC]_t$ was the observed mixing ratio of ith species and k_i was the correspondent rate constant with •OH.

3 Results and discussions

3.1 Meteorological variations and Mixing ratios

Meteorological conditions are important factors that impact both the compositions and levels of VOCs. During the sampling period, the T ~~(RH) was~~ varied from 15°C ~~(15%)~~ to 38°C ~~(100%)~~ (Fig.S1), and the dominant wind ~~was~~ northwestern and southeastern (Fig. 2). The air clusters, analyzed by HYSPLIT model, showed moderate differences in each month (Fig. 3). In May, clusters arriving at Zhengzhou demonstrated longer paths, and included six clusters in total, while in June, the length of clusters were shorter. However, the concentration levels and compositions of VOCs were similar in the two months. In May, the largest cluster (27.2%) was passed over from Yinchuan, a central city in northwest China, then crossing several non-capital cities (i.e., Yanan, Yuncheng and Luoyang) in Shanxi and Sichuan provinces. Such a long-range transport of pollutants ~~might result a~~ less impact on the air quality of Zhengzhou, as comparable level and

similar compositions of VOCs were obtained during the period of May - June. In June, August and September, approximately half of the air trajectories originated from the areas of Henan province, indicating the air pollutants in Zhengzhou were impacted by local factors ~~at most time~~.

The total concentrations of VOCs (Σ_{VOCs}) are presented in Table 1. The Σ_{VOCs} varied at the four sites, where the highest Σ_{VOCs} and their compositions were not identical across the sampling months as well. In May 2017, the highest Σ_{VOCs} was reported at JK (37.65 ± 22.58 ppbv), followed by GS (31.73 ± 18.70 ppbv), YH (30.05 ± 16.43 ppbv) and MEM (29.05 ± 15.34 ppbv), while the Σ_{VOCs} values for the month of June, July, August and September were found to be in the order of: GS>JK>MEM>YH, MEM>GS>JK>YH, YH>MEM>JK>GS, and MEM> YH > GS >JK, respectively. This can be attributed to numerous factors that will be explored later in the paper. Besides the emission sources (to be discussed in Section 3.2), the impacts controlled by meteorological conditions should not be ignored as well. For instance, the prevailing wind in May was northwestern at GS and YH, while the southwestern wind was dominant at JK (Fig 4). The transport of air pollutants from urban center and industrial plants should be resulted in the highest level of Σ_{VOCs} at JK. In June 2017, the prevailing wind was southeastern at MEM, YH and GS (Fig. 4). The average wind speed at GS (0.74 ± 0.33 m s^{-1}) was lower than that at MEM (1.84 ± 0.94 m·s^{-1}) and YH (0.97 ± 0.36 m s^{-1}) (Table 2), indicating poor dispersion conditions at GS. The air pollutants emitted from MEM and YH were more liable resulting in a higher level of Σ_{VOCs} at GS in June. It should be noted that, when Σ_{VOCs} at JK was higher than that of GS, the level at YH was higher than that of MEM, and vice versa. Except for the discriminations between the pollution sources at every site, the above phenomenon might be a result of the topography, where the elevation was gradually increased from east to west in Zhengzhou (Mu et al., 2016).

Due to the variations of the planet boundary layer (PBL) height, solar radiation and emission sources, the concentrations of VOCs displayed obvious differences between morning and afternoon time (07:00LT and 14:00LT in this study). Compared with morning period, the aromatic compounds showed lower compositions at14:00 LT (Fig. 5), because of the increased planet boundary layer and the active photochemical reactions, while alkenes always peaked in the14:00 LT. According to the dataset, the increases in alkene compositions (~4.3% uplift) were mainly due

to higher contributions of isoprene (~1.4% at morning and 7.6% in the afternoon), which was mainly emitted from biogenic sources and increased exponentially with ambient temperature (Jiang et al., 2018).

The average Σ_{VOCs} values in Zhengzhou (28.83 ± 22.05 ppbv) were significantly lower than those in Beijing (65.55 ppbv), Hangzhou (55.9 ppbv), Guangzhou (47.3 ppbv) and Nanjing (43.5 ppbv), and higher than that in Wuhan (23.3 ± 0.5ppbv) (Table 3). Factors, including population density, industrial activity, fuel composition, local stringent regulations for environmental protection, terrain, and weather are the potential reasons for the ~~discrimination of~~ VOCs concentrations in those cities. With regard to the weight percentage of major groups (Table 3), the composition of alkanes was the largest in all cities because of their longer lifetimes and widespread ~~from a variety of pollution~~ sources (Fig. 5), while the composition of aromatics was lower than alkenes in these cities except for Guangzhou. It is well known that aromatics mainly originate from solvent usage and vehicle exhaust in summer. The large amount of shoemaking and shipbuilding industries involving large amounts of solvent usage may be the main reason for the higher composition of aromatics in Guangzhou. In comparison with other four cities, the composition of aromatics in Zhengzhou was the lowest probably due to its less solvent-used manufacturers than in Guangzhou, Hangzhou and Nanjing, and less numbers of vehicles than in Beijing. Alkyne contributes least to VOCs in cities listed in Table 3, with higher level observed in Zhengzhou, where ranked second after Hangzhou. Alkyne typically originates from combustion sources. Zhu et al. (2016) observed that the composition of alkyne in the biomass-burning period could be double of that in the non-biomass burning period (Zhu et al., 2016). As Henan is the largest agricultural province in China and the sampling duration covered the crop harvest season, the residents often used crop residues as the biofuel for their subsistence and a higher alkyne composition in Zhengzhou was thus resulted.

3.2 Temporal variations

The time series of mixing ratios of NO_x, O_3 and Σ_{VOCs} at every site are shown in Fig. 6. The results showed a distinctive temporal characteristic where lower levels of SO_2, CO, NO_x, O_3 and Σ_{VOCs} were observed in July and August (mid-summer) (Table S5). These results were similar to

those obtained for other urban area (Li and Wang, 2012;Cheng et al., 1997;Na et al., 2001). Changes in PBL height, human activities, and abundance of hydroxyl radicals (•OH) were the potential causes for the phenomenon. Pal et al. (2012) reported that the PBL height was positively correlated with temperature. The occurrences of precipitation and raining were also frequent in most areas of China during summer, resulting in decreasing background level of air pollutants. Additionally, a series of effective local policies, such as prohibition of painting and coating in open air and limitations on fuel supply between 10:00 -17:00 LT during hot summer days assisted in suppressing the emissions of VOCs. Meanwhile, many organizations, such as schools, institutes and scattered private workshops, were closed due to summer vacations. Some large-scale industries also stopped manufacturing processes for two weeks during this period. Consequently, the anthropogenic emissions were reduced, which in turn resulted in a decrease in VOCs, SO_2, and NO_x emissions. The reduction of precursor levels and unfavorable photochemical conditions (such as, higher RH) resulted in the lower O_3 levels in July and August.

Beside local emissions, the long-range air mass also had some impacts on relatively lower level of Σ_{VOCs} in July. As illustrated in Fig.3, different from other months, the air current was originated with the largest portion (*ca.* 88.68%) of clusters from Hubei province, where the average Σ_{VOCs} in its capital city (23.3±0.6 ppbv) (Lyu et al., 2016) was lower than that in Zhengzhou (29.18±23.08 ppbv). In combination with the lower weight percentage of photothermal-reactive aromatics (10.30±4.23%), and the lowest toluene to benzene (T/B) ratio of 1.15±0.99 around this period, it is possible that the cleaner air mass clusters originating from Hubei also contributed to the reduction of Σ_{VOCs} in July.

As demonstrated in Fig. 6, the observed Σ_{VOCs} values at 07:00 LT were often higher than those at 14:00 LT. The accumulation of pollutants during night-time and the temperature inversion in the morning were the most reasonable explanations for this phenomenon. Stronger photochemical reaction during noon-time led to the reduction in atmospheric VOCs. It should be noted that pronounced Σ_{VOCs} were occasionally observed at MEM and GS (Fig. 7), which were potentially ascribed to sharp changes in local emissions and meteorological conditions. Specifically, at MEM, the distinctive increment was always accompanied with obvious increases of alkanes or aromatics

282 (Fig. 7). Since the T and RH were often consistent during the sampling period, the direct gas

283 evaporations should be constant as well. Therefore, the simultaneous increased concentrations of

284 SO_2, CO and NO_x could illustrate the potential impacts from combustion sources, such as emissions

285 from nearby thermal power plant. At GS, the increase of Σ_{VOCs} in June was usually with extremely

286 high levels of aromatics, due to the disturbance from solvent use for building renovation during this

287 period, and the abnormal high levels of Σ_{VOCs} in other months were related to the rising

288 concentrations of C_3-C_4 alkanes, which were mainly originated from consumptions of compressed

289 natural gas (CNG) or LPG (Huang et al., 2015). The results support the possible impact from a

290 gas-fueled power plant located about 1 km southwest of the site (~18% of prevailing western wind

291 at GS during May to September).

292 It is of interest to note that on the morning of 5th September, acetylene was found in extremely

293 high concentrations (14.65 - 39.42 ppbv). Its mixing ratio in most of the urban areas was <10 ppbv

294 (Louie et al., 2013;Duan et al., 2008;Guo et al., 2012). It was learnt that the 5th September is a

295 festival day for the people who worship their ancestors. A large number of incenses and offerings,

296 made up of wood and paper, were burnt during the festival, resulting in an elevation of acetylene all

297 over the Zhengzhou city (Zhu et al., 2016).

298 **3.3 Spatial variations**

299 The C_2 - C_5 alkanes, acetylene, ethylene, toluene and benzene were the most abundant VOCs

300 detected at all sites (Fig.8), and the mixing ratios of toluene varied within a wide range at each site,

301 because of its universal emission sources (e.g., vehicle exhaust emissions and solvent usage) (Wang

302 et al., 2014;Barletta et al., 2005). These chemicals contributed >60% for Σ_{VOCs} at each site,

303 illustrating strong combustion-related sources in Zhengzhou.

304 Among the four major organic classes, alkane was the most abundant group as a result of its

305 widespread sources and longevity (Fig.5), accounted for 52.9%, 62.5%, 53.4%, 53.4% of the total

306 Σ_{VOCs} at JK, MEM, GS, and YH, respectively. The highest composition of alkane was observed at

307 MEM due to the stronger contributions of ethane, iso-pentane, and C_6-C_8 branched alkanes (Fig.

308 S3), which are emitted from light-duty gasoline vehicles (Wang et al., 2017a).

The average Σ_{VOCs} were slightly higher at industrially impacted sites of GS (31.66±28.73 ppbv) and JK (28.63±22.04 ppbv) than those at MEM and YH (Fig.9). Additionally, the air pollutants related to the combustion processes, such as SO_2 and CO, were more abundant~~, though marginal,~~ in western area of Zhengzhou (GS and MEM) (Fig.9). Under high levels of VOCs and sufficient supply of NO_x, the highest average mixing ratio of O_3 was observed at GS, followed by YH where even with the lowest VOCs and NO_x, indicating that there are multiple factors, rather than the absolute concentrations, contributed to the O_3 ~~formation~~ at YH.

In June, the O_3 concentration often exceeded the national standard level of 80 ppbv, ~~representing~~ severe air pollution during this period. The average mixing ratio of O_3 during daytime (07:00-18:00 LT) in June, 2017 at JK, MEM, YH, and GS were 74.87±39.55 ppbv, 73.50±40.59 ppbv, 73.81±35.69 ppbv, and 87.99±46.11 ppbv, respectively (Table 4). The higher level of O_3 at GS was accompanied with the higher Σ_{VOCs} (39.29±25.37ppbv). The weight percentage of aromatics (15.62±12.06%) at GS was higher than those at other sites as well, indicating that the painting and other renovation activities at GS was potentially an important factor for its high O_3 level in June. Even though both the Σ_{VOCs} and specifically high O_3 formation potential compounds (such as alkenes and aromatics) at MEM were slightly higher than those at YH (Table 4), the O_3 concentration at MEM was not higher. This could be attributed to other critical precursors such as NO. NO at MEM (7.72ppbv) was significantly higher than that at YH (2.57 ppbv) during daytime, indicating that the titration reaction between O_3 and NO was more efficient at MEM.

~~It is well known that many~~ O_3 episodes ~~were~~ attributable not only to local sources but also to regional transport~~s~~. For example, Streets et al. (2007) reported that with continuous southern winds, the O_3 level in Beijing was 20-30% contributed from its neighboring cities in Hebei. During ~~this~~ study, a typical regional ozone pollution ~~was~~ happened on August 10th at YH (Fig.6). On that day, the ratios of Σ_{VOCs}/NO_x at the four sites were all less than 6.5 (ppbC/ppbv) (Fig. S4), indicating a regional VOC-control system, and that VOCs are the critical contributors to the formation of O_3 in Zhengzhou. The reductions in Σ_{VOCs} in the afternoons (around 14:00 LT) compared to mornings (around 07:00 LT) may have been ~~caused from the uptake~~ by O_3 formation, while ~~t~~he reduction of Σ_{VOCs} and active compounds (i.e., aromatic+alkene) at 14:00 relative to 07:00, ~~determined as~~ 35%

337 and 56% respectively, ~~were the~~ least at YH among the four sites (Fig. S4). ~~On the other hand,~~ based

338 on the ~~dispersion of~~ wind direction, between 08:00 - 15:00 LT on August 10th, YH was ~~at the~~

339 downwind ~~position to~~ the other three sites (Fig. S4). All of this confirmed that the abnormally high

340 O_3 at YH was caused by the transport of air pollutants from other sites on that day.

3.4 VOCs/NOx ratio

342 The VOCs/NO_x ratio is often used to distinguish whether a region is ~~VOCs~~ VOC or NO_x limited in

343 O_3 formation. ~~According to the general case,~~ ~~the area was~~ ~~loaded in~~ VOC-sensitive ~~regimes when~~

344 VOCs/NO_x ratios ~~were~~ lower than 10 in the morning; ~~and it would be on~~ NO_x-sensitive regime

345 when VOCs/NO_x ratios ~~were~~ greater than 20 (Sillman, 1999;Hanna et al., 1996). In this study, the

346 mean value of VOCs /NO_x (ppbC/ppbv) were below 5 at all four sites (Fig.10), and 75% of the data

347 points were < 6, indicating that the O_3 formation was sensitive to VOCs in Zhengzhou, and the

348 reductions on the emissions of VOCs will be benefit for O_3 alleviation.

349 The VOCs /NO_x showed differences among the four sites (Fig. 10), with the lowest value at

350 MEM (~3.8) and the highest value at JK (~4.7). The ~~distributions demonstrated that the~~ production

351 of O_3 at MEM ~~was~~ more sensitive to VOCs than JK due to presence of emission from

352 thermal-power plant. ~~Meanwhile,~~ approximately 14% of the VOCs /NO_x ratios of >8.0 were found

353 in the NO_x-limited site of JK, ~~potentially~~ resulting from higher VOCs or lower NO_x emissions than

354 other sites. Both of the mixing ratios and the statistical data showed higher levels of VOCs (with

355 lower NO_x) at GS, where only ~4% of the ratios of > 8 was observed, indicating that there must be

356 other factors (unresolved in this study) impacted the variation of O_3 formation regimes.

357 From the daily variations of VOCs /NO_x ratios (Fig. 10), higher values were observed at 14:00

358 LT than 07:00 LT at ~~the~~ four sites, well correlated with less vehicle emissions or more consumption

359 paths for NO_x with stronger light intensity. The increment of VOCs /NO_x at 14:00 LT was more

360 obvious at JK and GS, suggesting that more emission sources of VOCs at daytime, and resulting the

361 O_3 formation system shifting to the transition area in the afternoon.

362 ~~Many researches showed that the~~ O_3 formation depends not only on the abundances of

363 precursors (mainly VOCs and NO_x) and also VOCs to NO_x ratio (Pollack et al., 2013). In this

research, the mixing ratio of O_3 at 14:00 LT presented a slightly positive trend (p<0.05) with the uplift of VOCs /NO_x at JK (Fig. 11), consistent to the results observed at the megacity of Shanghai (Gao et al., 2017), where the O_3 formation was more sensitive to NO_x when high O_3 levels were observed. This can be attributed to the increased O_3 production efficiency at high VOCs /NO_x. There were no discernible trends at other sites, possibly due to the counteraction imposed by other uncertain factors.

3.5 Ratios of specific compounds

Ratios of specific VOCs are useful ~~indicators~~ to identify ~~the~~ emission sources (Raysoni et al., 2017;Liu et al., 2015;Ho et al., 2009). In order to characterize the differences in the contribution of various sources at each site, ~~two~~ ratios of i-pentane/n-pentane and ~~T/B~~ ratios are discussed.

The ratio of i-pentane to n-pentane can be used to differentiate potential sources such as consumption of natural gas, vehicle emissions and fuel evaporations. ~~It is claimed that in~~ areas heavily impacted by natural gas drilling, the ratios ~~were~~ lied ~~within~~ the range of 0.82 - 0.89 (Gilman et al., 2013;Abeleira et al., 2017). Higher values ~~were~~ often reported for automobiles, in a range of 2.2 - 3.8 for vehicle emissions, 1.8 - 4.6 for fuel evaporation, and 1.5 - 3.0 for ~~gasoline~~ (Russo et al., 2010;McGaughey et al., 2004;Jobson et al., 2004;Wang et al., 2013), whereas the ratios below unity was found for coal combustion (0.56 - 0.80) (Yan et al., 2017).

In this study, i-pentane and n-pentane were highly correlated (R^2=0.87 - 0.94) throughout the whole sampling campaign (Fig. 12), indicating constant pollution sources for these two compounds. The highest ratio of i/n-pentane was found at JK (2.59), which was comparable to the value of 2.93 reported in a Pearl River Tunnel (Liu et al., 2008), thus indicating strong impacts from traffic-related sources. The average ratio at MEM was 2.31, higher than the character ratios of coal combustion, reasonably due to the observation site presented at upwind position of the thermal power plant. Additionally, it is remarkable that MEM was surrounded by a main road with four traffic lanes. The distance between the nearest traffic light and the sampling site was just 200 m. Frequent idling may cover up the contribution from coal combustion, reflecting the impact of traffic

emissions. The average ratios at YH (1.94) and GS (1.63) were lower than those at the above two sites, suggesting the comparatively stronger contribution from coal burning.

~~The T/B ratio is another efficient tool to differentiate pollution sources. Both the~~ tunnel and roadside research~~es~~ indicated that T/B ratio varied within the range of 1 - 2 when the atmosphere ~~was~~ heavily impacted by vehicle emissions (Gentner et al., 2013;Tang et al., 2007;Huang et al., 2015;Wang et al., 2002). The ratio of <0.6 was ascribed to other sources such as coal combustion and biomass burning (Tsai et al., 2003;Akagi et al., 2011). The industrial activity would be more dominant when the T/B ratio is greater than 3 (Zhang et al., 2015).

In this study, the correlation between benzene and toluene was fairly well at all the sites (R^2=0.70-0.74), except for YH (R^2=0.41) (Fig.14), suggesting the similar sources for benzene and toluene at JK, MEM and GS, while more complex such as variable wind direction at YH. The average ratios of T/B were lied within the range of 1.64-2.29, which were scattered around the character ratio of 2 for vehicle exhaust, illustrating the significance of vehicle emissions at the four sites. Specifically, at JK, MEM and YH, most of T/B ratios were distributed between 0.6 and 3, which were corresponding to character ratios for coal or biomass burning and industrial activities respectively. These reflected the mixture impacts from mobile source and coal/biomass burning at these three sites. However, more values were greater than 3 at GS, suggesting more frequent disturbance from industrial activities at this site.

~~From the temporal respect,~~ the T/B ratios at 14:00 LT were lower than at 07:00 LT (Fig.15). ~~In fact,~~ the reaction rate constant of toluene (5.63×10^{-12}cm^{3}molecule^{-1}s^{-1}) with •OH is ~~much~~ higher than that for benzene (1.22×10^{-12}cm^{3}molecule^{-1}s^{-1}), ~~representing~~ more rapid consumption of toluene from photochemical reactions and thus resulting in lower T/B ratios at 14:00 LT. ~~Besides,~~ the emission strength of mobile source is often weaker at 14:00 LT, while the coal/biomass burning are increased due to more human activities. Both ~~of the situations can be used to explain~~ the lower T/B ratios observed at 14:00 LT. In comparison with other months, higher T/B ratios were found more frequently in September, potentially showing ~~the more strengthen indusial~~ activities during this period.

Overall, based on the iso-pentane/i-pentane and T/B ratios, the atmospheric VOCs at every site were impacted by a mix of coal/biomass burning and vehicle emissions, whereas GS was more liable impacted by industry-related sources.

3.6 Relative reactivity of VOCs

The reactivity of individual species ~~was~~ different, ~~while~~ mixtures of VOCs ~~would have~~ competition ~~the precursors between each other~~, leading to variations ~~on~~ reaction ~~paths~~ and O_3 formation yields. Ozone formation potential (OFP) is a useful tool to estimate maximum O_3 production~~s~~ of each compound under optimum conditions, from which the ~~vital~~ species ~~in~~ O_3 formation could be identified (Huang et al., 2017). The calculation of OFP is based on mixing ratios and maximum incremental reactivity (MIR) of individual compound, ~~which are expressed in~~ Eq. (4).

$$OFP=C_i \times MIR \qquad (4)$$

where C_i represents the concentration level of ith species, while *MIR* is a constant taken from Carter (2010) (Table S1).

In Zhengzhou city, alkenes contribute most ($55.91 \pm 14.17\%$) to the sum of OFP, of which ethylene had the largest portion. The results is different with the estimation based on emission inventories by Wu and Xie (2017), in which the largest contributor of total OFP in North China Plain (NCP), YRD and PRD was aromatics, reflecting that there was relatively less surface coating industries in Zhengzhou.

For the individual species, the top 10 most contributors in OFP included ethylene, isoprene, m,p-xylene, toluene , propylene, acetylene, n-butane, i-pentane and propane. Their contributions to the sum of OFP was lied within the range of 69.44 - 77.60% (Table 5), with 61.30-76.46% of total VOCs weighted in concentration, highlighting the importance of reduction on emissions of these VOCs no matter based on relative reactivity or mixing ratios. Additionally, it is worth noting that, the percentage of acetylene ($4.51 \pm 0.34\%$) weighted in OFP was higher than many other areas in China, including Guangzhou (2.20%) and YRD (2.37%) (Li and Wang, 2012;Jia et al., 2016),

demonstrating that it is necessary to conduct emission controls on sources related to combustion (i.e., vehicle emissions and biofuel burning) in Zhengzhou city .

Zhengzhou was suffered from the severest O_3 pollution in June, 2017. The relationships between OFP of each organic group, $\Sigma_{VOCs,}$ and the ambient concentrations of NO_x and O_3, as well as the corresponding meteorological conditions, are shown in Fig. S5-6. At 07:00 LT, generally lower WS was seen than that at 14:00 LT, offered a favorite condition for local O_3 propagation. Under low RHs and high T and OFP (88.13 ± 30.32 ppbv), the O_3 level at YH was unexpectedly lower than that at MEM on sunny days. Since the OFP was estimated with the assumption of reactions that proceeded under optimum conditions, the above phenomenon reflected there were unsatisfied O_3 formation conditions at YH. The highest total OFP was seen at JK in June, while the highest O_3 levels was observed at GS where located at a downwind position with lowest WS (0.74 ± 0.33 m s^{-1}). The concentration level of O_3 usually increased with wind speed (Fig.S7), particularly when the eastern wind was dominant, illustrating the disturbance from long-distance sources to urban center.

3.7 Source apportionment

The factor profiles given by PMF for each site were presented in Fig.15. The six factors were resolved as vehicle emissions, coal+biomass burning, solvent use, oil evaporation, petrochemical and biogenic source (detailed characterization can be referred to supporting information) on the base of the correspondent markers for each source categories, which were summarized in Table S6. Meanwhile, the correlation coefficients, expressed in Pearson's r, were varied from 0.54 to 0.62 and 0.66 to 0.73 for SO_2 with coal+biomass burning, and NO_2 with vehicle emission, respectively (Fig. 16), proved the precise results gained in this study.

The weight percentage of each factor calculated with two criteria (absolute concentrations and OFPs) at the four sites were presented in Fig.17. At every site, vehicle emission, coal+biomass burning and solvent use were the top three contributor to VOCs abundance in ambient air. Compared to JK and YH, even though the distances between thermal power plant and the observation site was the shortest at MEM, vehicle emission (36.82%) showed the largest portion

instead. Coal+biomass burning (30.58%) had the highest contribution at GS, attributed to its downwind position and nearby suburbs that biomass burning occurred more frequently. The contributions from vehicle emission at the two urban centers of MEM (36.82%) and YH (37.39%) were comparable, but higher than those at JK and YH. The consumptions of solvent at GS (18.86%) and JK (14.95%) were higher than those at YH (10.1%) and MEM (11.48%), due to restriction on development of new industrial enterprises in urban center in recent years. Emissions from oil evaporation, petrochemical and biogenic emission were scarce, and their contributions were below 10% at every site.

On the base of O_3 formation impact, coal+biomass burning, solvent use, and vehicle emission were the three major contributors as well. In contrast to the concentration weighted method, the importance of solvent use estimated with OFP increased 28-65% for each site, and the significance of vehicle emissions decreased 29-53%. At YH and GS, small discrimination (<4%) in contributions of coal+biomass burning between the two methods were found. On the other hand, the variations on coal+biomass burning at JK (a decline of 17%) and MEM (an increase of 29%) were more obvious, due to low abundance of reactive species in this factor at JK and high level of alkenes at MEM. Considering that the aging index of xylene/ethylbenzene was high at MEM (2.97) and low at JK (0.01) remarkably, demonstrating that the emission sources related to coal+biomass burning was fresher at MEM than JK.

Except for oil gas evaporation and biogenic sources, in which major emitted compounds with shorter life span, potential source regions for the other four identified sources (i.e., coal+biomass burning, vehicle emission, solvent usage and petrochemical) apportioned by PSCF method were presented in Fig. 18. Southwest of Shanxi province, western of Shandong province, and southwest of Henan province were identified as hot spots for the coal+biomass burning. The active emission areas for solvent use were concentrated in Henan province, and mainly located in southwest of Zhengzhou. The most contribution area for petrochemical was found in southwest of both Shanxi and Henan, northwest of Anhui, and southeast of Hubei provinces. For vehicle emissions, the strongest emission point was scattered in southwest of Henan, while Shandong, Anhui and Hubei provinces also distributed with strong emission points.

3.8 Consumption of VOCs and correlations with ozone level

The consumption of a VOC in the atmosphere could be presented as the difference from its initial mixing ratio and the observed value. The groups of alkenes and aromatics had larger consumption than alkanes, particularly at JK and GS (Fig.19), which was consistent to stronger impacts from solvent usage at the two sites.

The average value of VOC consumption at urban center (MEM and YH, 4-6ppbv) was lower than that at marginal area (JK and GS, 9-11ppbv), and the average increment of O_3 at 14:00 LT was higher than that at 07:00 LT in marginal area, suggesting more efficient photochemical reactions at JK and GS. Meanwhile, the average values of $[\cdot OH]\triangle t$ for each site, ranked in the same order with VOCs consumption, were varied in a range of 2.9×10^{10} to $4.71\times10^{10} cm^{-3}$ s. The values were slightly lower than the results of $4.9\times10^{10} cm^{-3}$ s measured at Beijing in August-September, 2010 (Yuan et al., 2012), indicating that comparatively less aging process in Zhengzhou.

Taken the decrement of VOCs and NO_x as independent variable and the increment of O_3 as dependent variable, the multiple regression analysis was performed. The results for JK and GS were presented as:

$[O_3]_{increment}=0.41[VOC]_{decrement}+0.20[NO_x]_{decrement}+53.44$ (JK, $R^2=0.44$)

$[O_3]_{increment}=0.34[VOC]_{decrement}+0.39[NO_x]_{decrement}+59.29$ (GS, $R^2=0.38$)

The F values for JK and GS were 16.1 and 10.1 respectively, indicating the regression results at the two sites were acceptable. However, the relationships among O_3, NO_x and VOCs could not be expressed in this way at MEM and YH, where the low values for both R^2 (0.12, 0.09) and F values (2.7, 2.8). This potentially attributed to more constant disturbance from fresh emission sources at urban center.

4. Conclusions

In this study, VOC samples were collected at four sites in Zhengzhou, Henan (China) for the first time and analyzed for 57 species. It is found that the weighted percentage of aromatics was lower, while alkyne was higher in Zhengzhou city than in other Chinese cities. C2 - C5 alkanes,

acetylene, ethylene, toluene and benzene were the most abundant VOCs in the region, suggesting widespread combustion-related sources in the city. On the basis of monthly average, the maximum Σ_{VOCs} was observed at GS site, where occasionally impacted from the nearby gas fueled plant. Approximately 75% of VOCs/NO_x ratios were below 6 at each site, indicating that the O_3 formation was driven by VOCs regionally. Different from other megacities, alkenes were the biggest contributors to OFP, and acetylene was particularly critical at each site. In addition, the impact of aging process was less in Zhengzhou than that Beijing. The photochemical reactions at JK and GS were more efficient, while the relationships among O_3, NO_x and VOCs at urban sites of MEM and YH were more complex. Either the mixing ratios or calculated OFPs demonstrated that the most important contributors to VOCs were vehicle exhaust, coal+biomass burning and solvent use, illustrating the necessary to conduct emission controls on these pollution sources. Vehicle emission was more dominant at urban center (YH and MEM), while solvent use was more important at the sites (JK and GS) far away from urban center in Zhengzhou. It is further shown that the air pollution in Zhengzhou was mostly impacted by local emissions according to the cluster analysis, and southern air clusters occasionally from Hubei Province was cleaner. In addition, strong emissions for coal+biomass burning were concentrated in southwest of Shanxi, western of Shandong and southwest of Henan provinces according to the PSCF analysis. Due to less anthropogenic emissions and more favorable dispersion conditions, most of the air pollutants had the lowest levels in the mid-summer month of July. This study provides the first-hand information on the characteristics of VOCs and assists in overcoming the O_3 pollution issue in Zhengzhou city, China.

Acknowledgements

This research was supported by the Key Program of National Natural Science Foundation of China (Grant No. 91744209).

548 **Table & Figure**

549

550 Table1. Concentrations of Σ_{VOCs} (ppbv) at every site during the sampling period

	JK		MEM		GS		YH	
	Mean	Std.	Mean	Std.	Mean	Std.	Mean	Std.
May.2017	37.65	22.58	29.30	15.34	31.73	18.70	30.05	16.43
June.2017	34.02	19.89	30.28	12.77	39.29	25.37	28.33	11.94
July.2017	16.01	6.13	20.74	12.66	19.60	13.94	15.95	7.54
Aug.2017	21.54	15.29	24.37	20.79	20.49	15.67	26.03	17.01
Sept.2017	26.20	16.22	34.15	23.85	30.36	19.76	32.56	19.76

551

552 Table2. Wind speed ($m \cdot s^{-1}$) at every site during the sampling period

	JK	MEM	YH	GS
May	1.34±0.65	1.86±1.19	1.27±0.66	0.97±0.49
June	1.07±0.48	1.86±0.94	0.97±0.36	0.74±0.33
July	1.48±0.59	2.62±1.19	1.15±0.45	0.90±0.32
August	1.06±0.48	1.86±0.94	0.95±0.39	0.76±0.35
September	0.80±0.38	1.24±0.80	0.82±0.43	0.62±0.38

553

554

555 Table3. Concentration levels of VOCs and compositions of major groups in Zhengzhou and other cities in China

Items		Guangzhou	Nanjing	Beijing	Hangzhou	Wuhan	Zhengzhou
		March-December, 2005	2011-2012	August, 2006	July-August, 2013	2013-2014	May-September, 2017
Sampling site		residents-commercial-transportation mixed area	transportation-industry mixed area	residents-commercial mixed area	residents-transportation mixed area	urban	urban
Quantified compounds		59 NMHC	56 NMHC	47 NMHC	56 NMHC	99 VOCs	56 NMHC
Total samples		145	_	24	_	_	400
TNMHC (ppbv)		47.3	43.5	65.55±17.44	55.9	23.3±0.5	29.18±23.08
Compositions of major groups (%)	*alkane*	49.0	45.0	52.3	33.2		56±12
	alkene	16	25.3	21.2	25.9		16±7.6
	aromatic	23	22.3	18.1	24.3		14±8.4
	alkyne	12	7.3	8.4	16.6		13±6.7
Reference		(Li and Wang, 2012)	(An et al., 2014)	(Guo et al., 2012)	(Li et al., 2017b)	(Lyu et al., 2016)	this study

556

557

558

559

560

561

Table4. Specific information on VOCs, O_3 and NO at the four sites in June, 2017

Composition or conc.	JK	MEM	YH	GS
Aromatic (%)	9.06	11.57	4.72	15.75
Alkene (%)	6.36	4.13	5.52	5.47
Σ_{VOCs} (ppbv)	34.02	30.28	28.33	39.29
O_3(ppbv)	74.87	73.50	73.81	87.99
NO(ppbv)	7.10	7.72	2.34	4.47

562

563

564

565

566

567

568

569

570

571

572

573

574

575

576

577

578

579

580   Table5. Top 10 VOCs ranked according to calculated ozone formation potential (OFP) and their corresponding

581   percentage weighted in mixing ratio

Site	Species	OFP (ppbv)	Weighted in OFP (%)	Weighted in mixing ratio (%)	Site	Species	OFP (ppbv)	Weighted in OFP (%)	Weighted in mixing ratio (%)
JK	Ethylene	18.99	25.54	8.22	MEM	Ethylene	18.44	30.88	7.92
	Isoprene	12.99	21.83	7.31		Isoprene	4.66	10.10	2.36
	m/p-Xylene	6.08	5.89	2.67		Toluene	3.73	6.67	3.99
	Toluene	5.53	5.83	4.22		Propylene	3.60	6.16	1.25
	Propylene	4.03	5.36	1.29		Acetylene	2.82	5.00	12.19
	Acetylene	2.97	4.44	13.54		m/p-Xylene	2.55	4.20	1.40
	n-Butane	2.15	3.05	7.28		n-Butane	1.81	3.20	5.97
	o-Xylene	1.83	2.00	0.88		Isopentane	1.76	3.16	7.39
	Isopentane	1.66	1.95	6.50		Ethane	1.58	2.96	23.35
	Propane	1.17	1.73	9.77		Propane	1.31	2.48	10.64
YH	Ethylene	19.83	28.10	8.88	GS	Ethylene	18.04	25.96	7.51
	Isoprene	7.44	11.30	3.67		Isoprene	8.01	16.75	4.64
	Toluene	6.63	7.75	5.72		Toluene	7.43	7.67	5.49
	m/p-Xylene	3.93	4.38	1.58		Propylene	4.39	5.85	1.26
	Acetylene	3.15	4.38	13.91		m/p-Xylene	4.31	4.57	1.75
	Propylene	3.01	3.60	0.91		Acetylene	2.76	4.24	12.07
	Trans-2-pentene	2.25	2.94	3.43		n-Butane	1.82	2.93	6.39
	n-Butane	1.84	2.80	6.31		Isopentane	1.71	2.68	6.94
	Isopentane	1.59	2.22	6.69		Propane	1.38	2.26	11.61
	Propane	1.18	1.98	10.20		Isobutane	1.13	1.98	4.59

582   [a] *m*-Xylene and *p*-Xylene are co-eluted in the chromatographic separation.

583

584
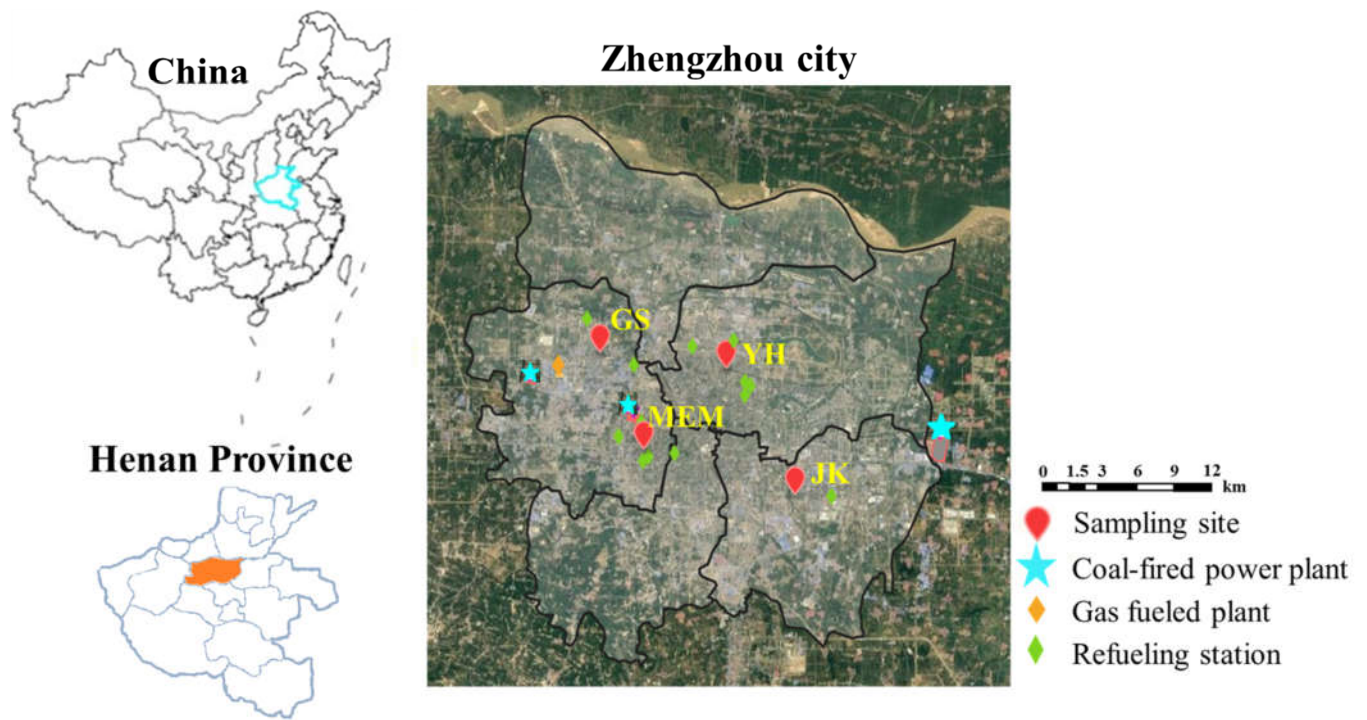
585

586   Fig 1. Map of Zhengzhou, China showing the locations of sampling sites.

587
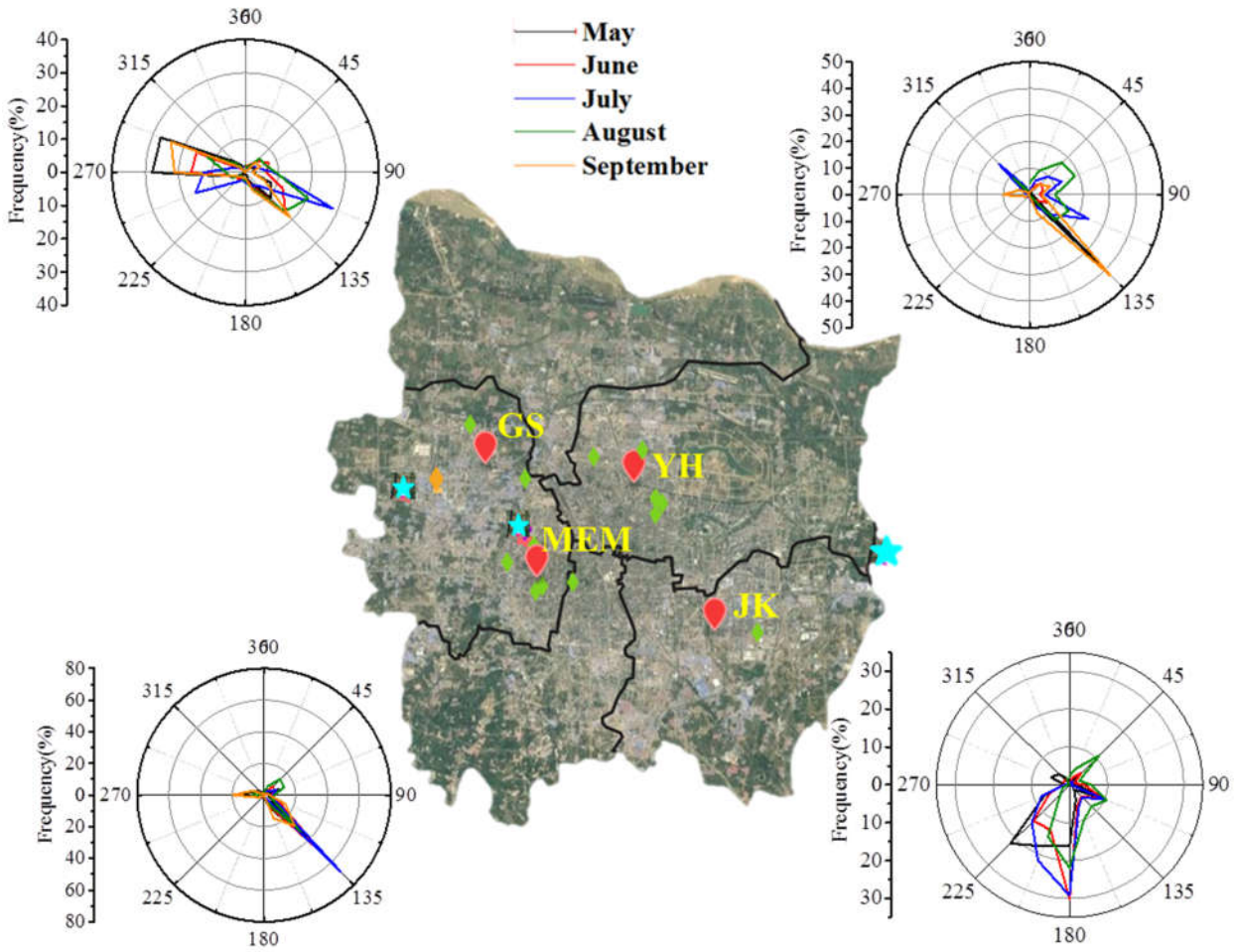
Fig.2 Wind direction for each site during May to September, 2017
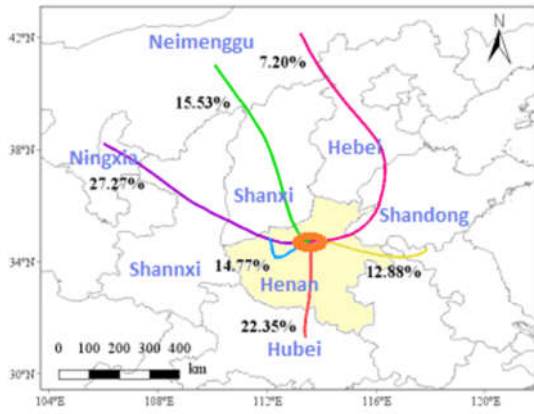
May   June
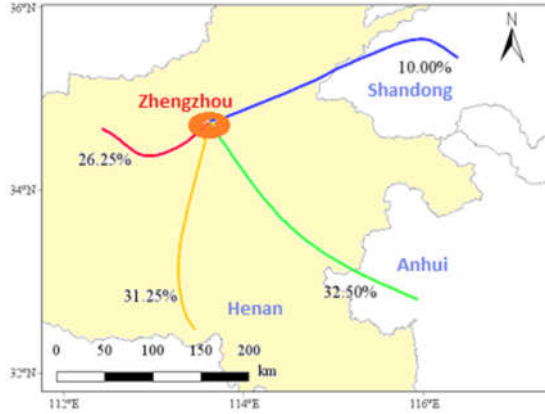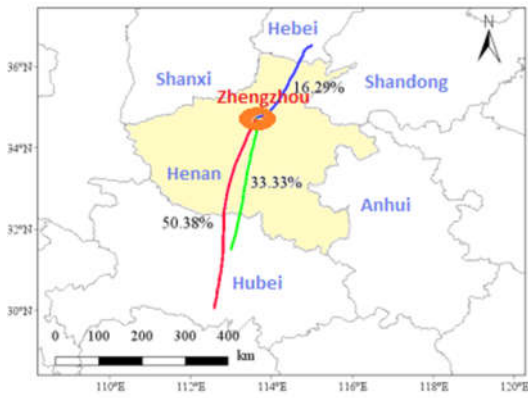
July   August
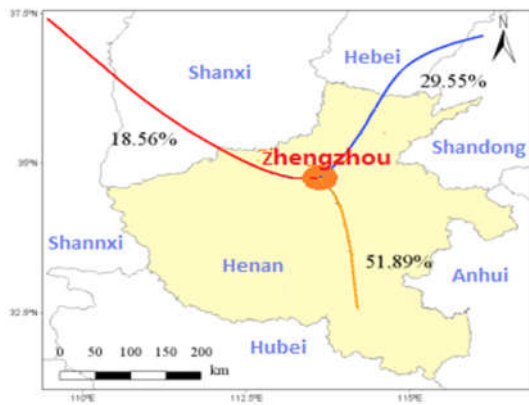
September
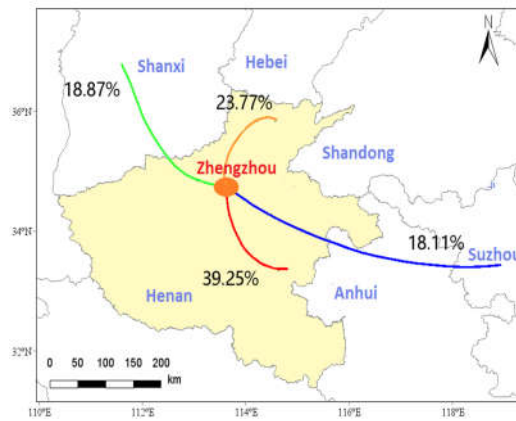
591   Fig. 3 Cluster analysis of Zhengzhou in each sampling month
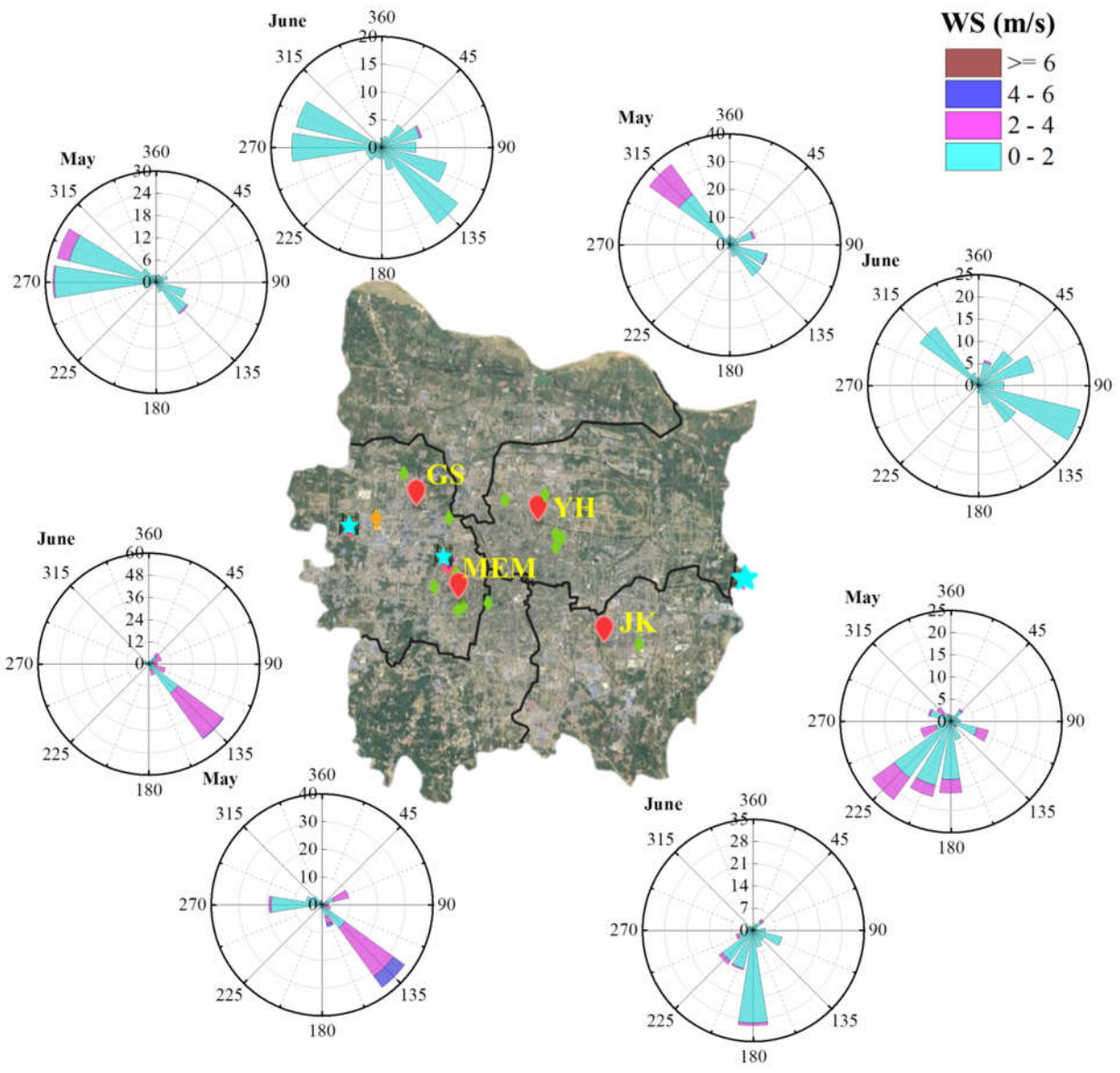
592

593   Fig.4 Wind rose at each site in May and June (the wind distribution in other three months were illustrated in Fig

594   S2)

595

596

597
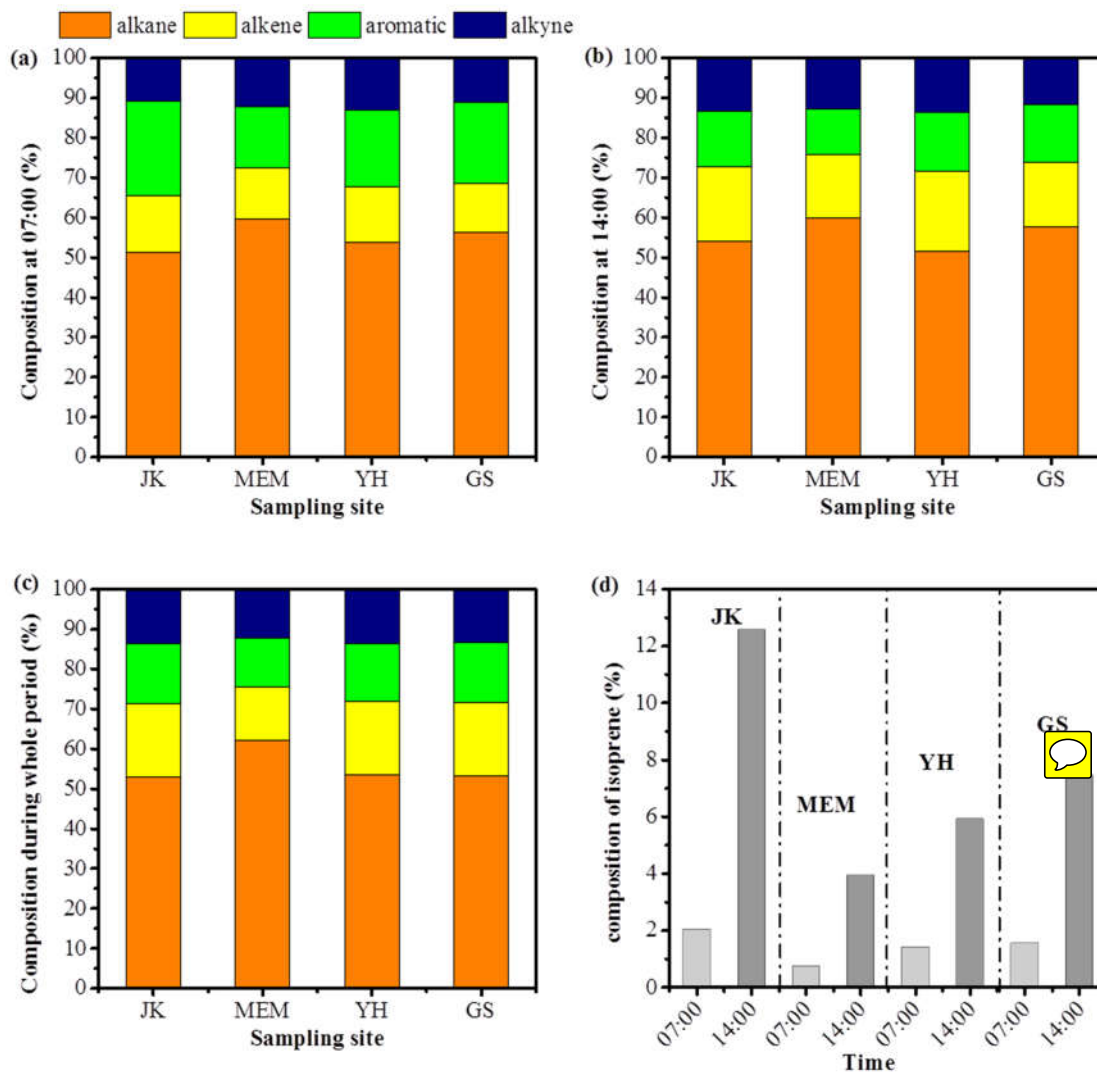
Fig. 5 Compositions of major organic classes at 07:00 LT (a), 14:00 LT (b) and during the whole sampling period

(c) at the four sites, and the composition of isoprene at 07:00 LT and 14:00 LT for each site (d).

600
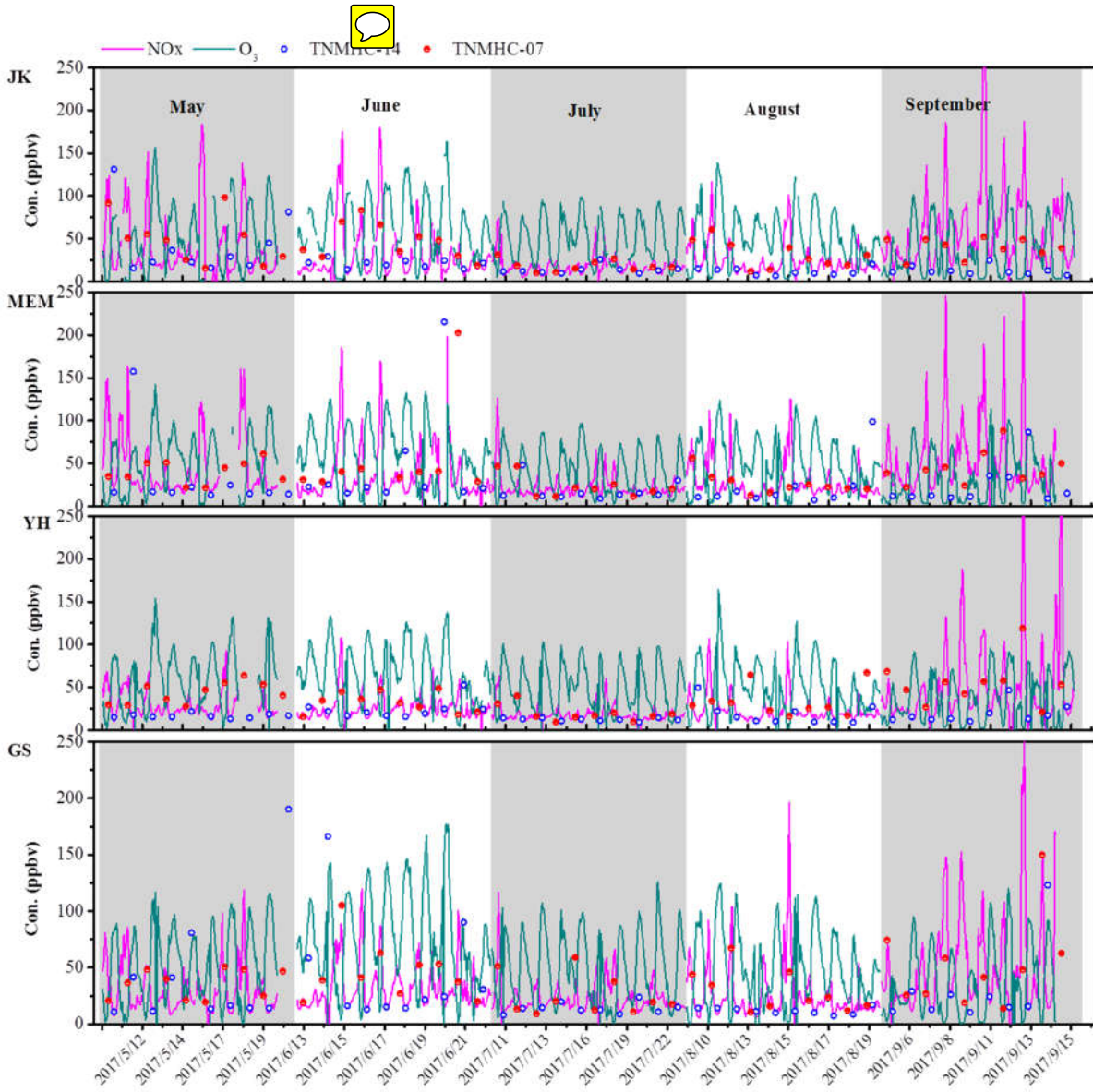
Fig.6 Temporal variations of mixing ratios of $\Sigma_{VOCs,}$ NO$_x$ and O$_3$ at the four sites during the whole sampling period, in which Σ_{VOCs}-07 stands for the concentration level of Σ_{VOCs} observed at 07:00 LT, and Σ_{VOCs}-14 was that observed at 14:00 LT.

607
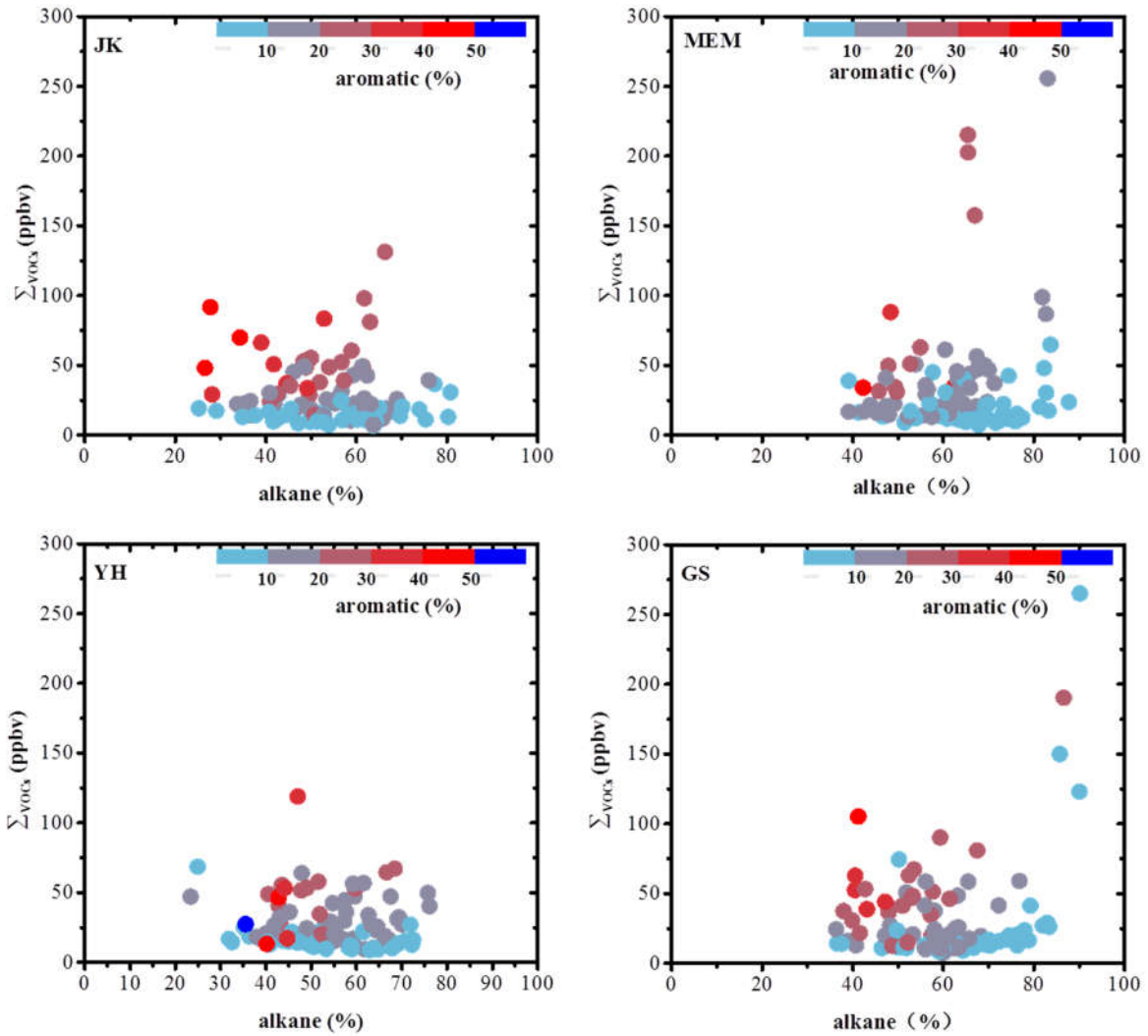
Fig. 7 The relationship between mixing ratio of Σ_{VOCs} and the composition of alkane, the data points ~~were~~ color coded with the composition of aromatic.

609

610

611
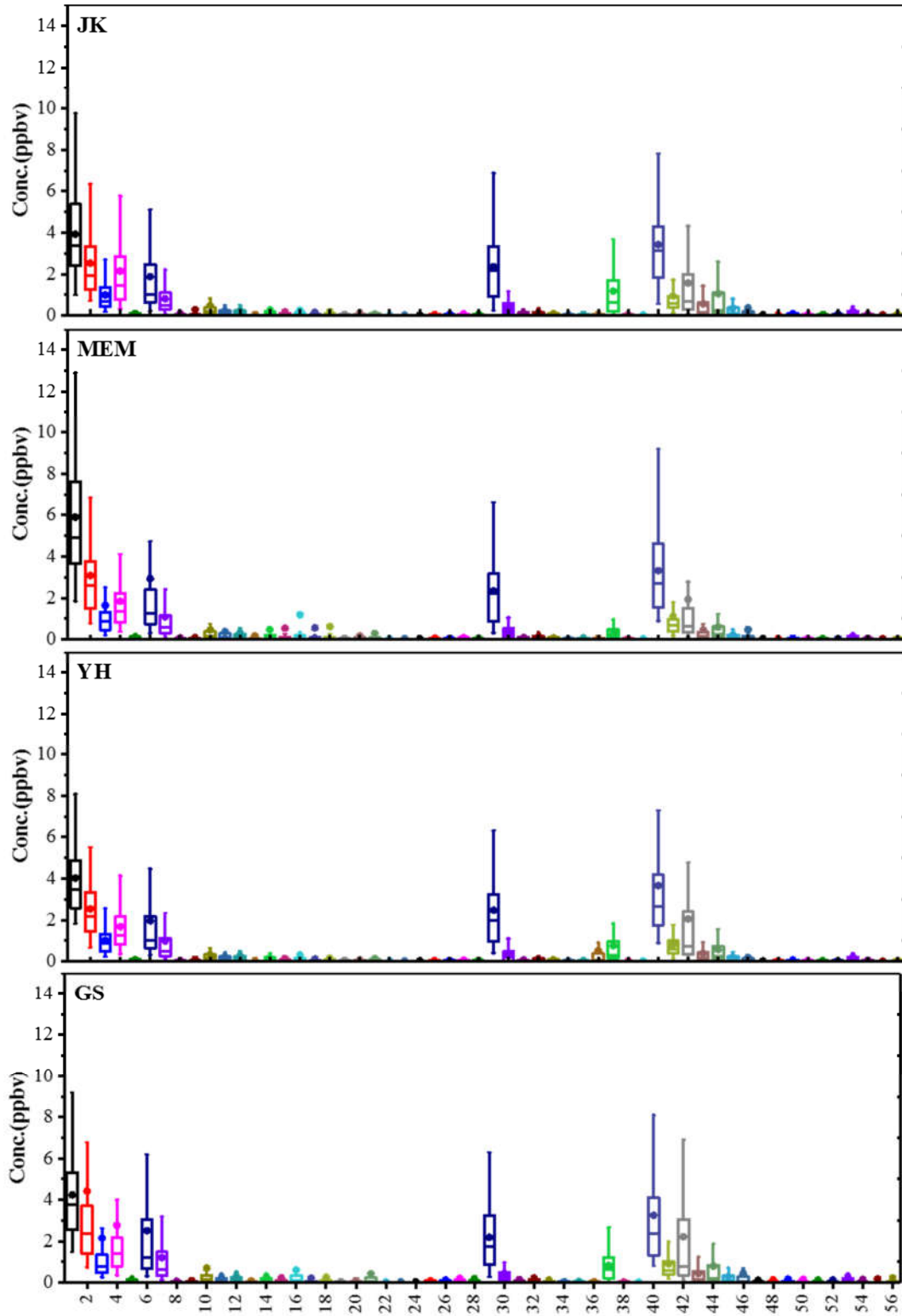
Fig.8 Concentrations of 57 VOCs at each site for the whole sampling period, the whisker was ranged from 5-95%,

and the box was 25-75%, the solid points stand for average value, the line in the box represent median value. The

number of chemicals can refer from Table S1.
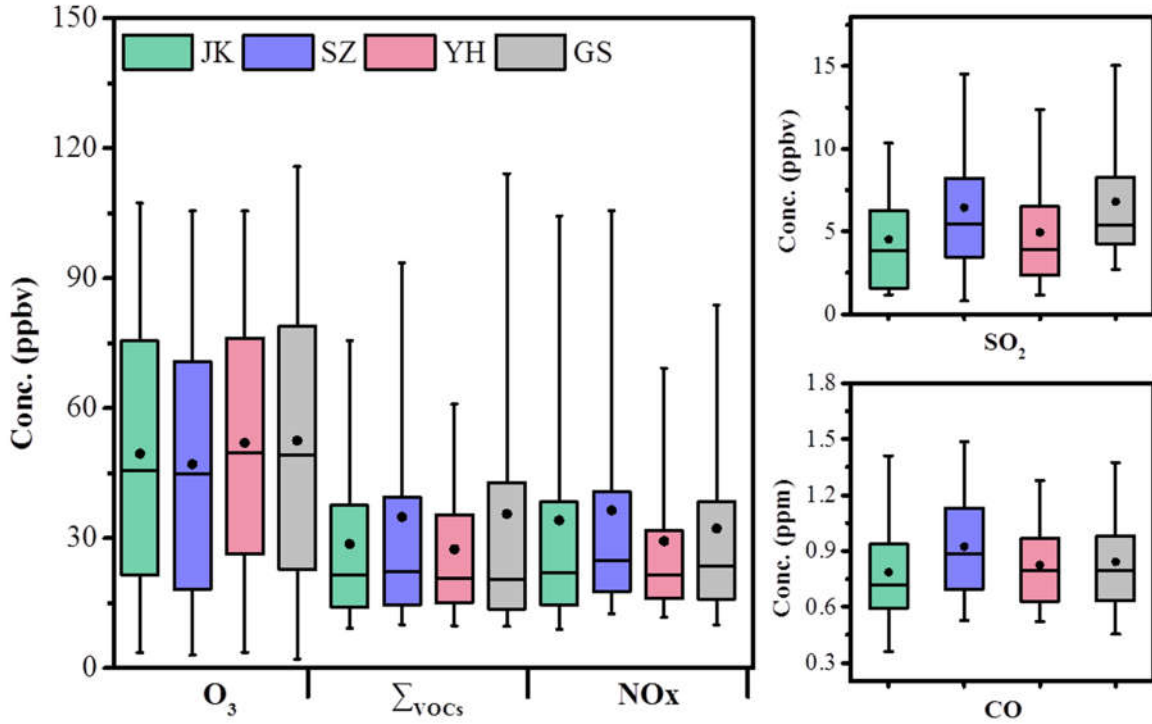
Fig. 9 The distribution of concentration point on O_3, Σ_{VOCs}, NO_x, SO_2 and CO at each site, the range of the box was 25%-75%, the black line in the box stands for median level, the black dot represent the average level, the range of whisker was 5-95%.
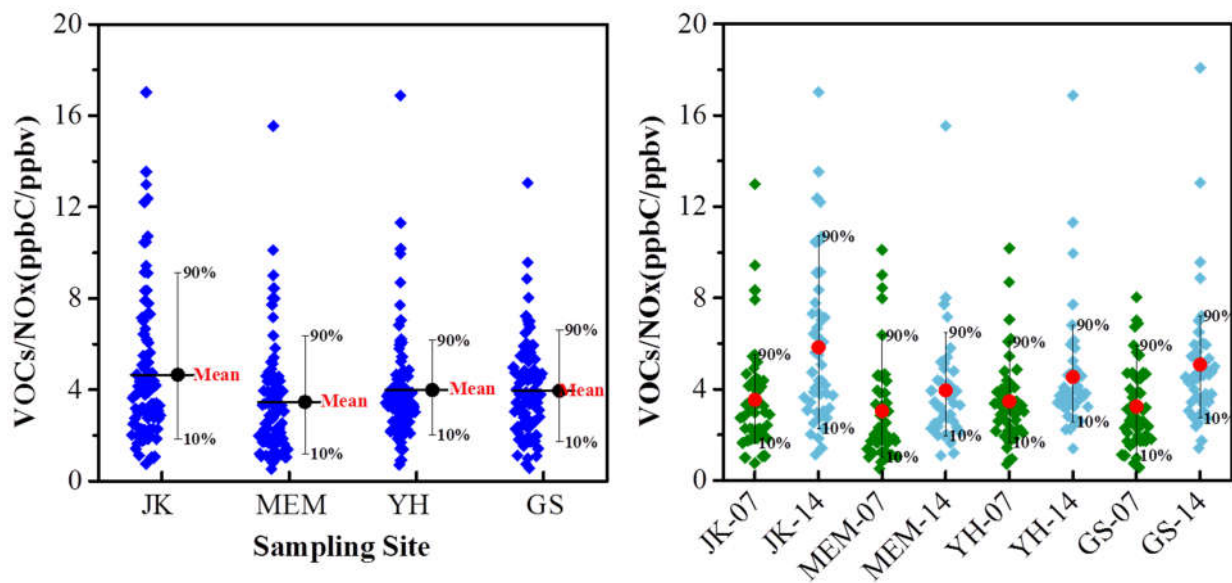
620

621   Fig.10 The data distribution of VOCs/NO$_x$(ppbC/ppbv) at the four sites (left), and the ratio observed at 07:00 LT

622   and 14:00 LT were presented (right).

623

624
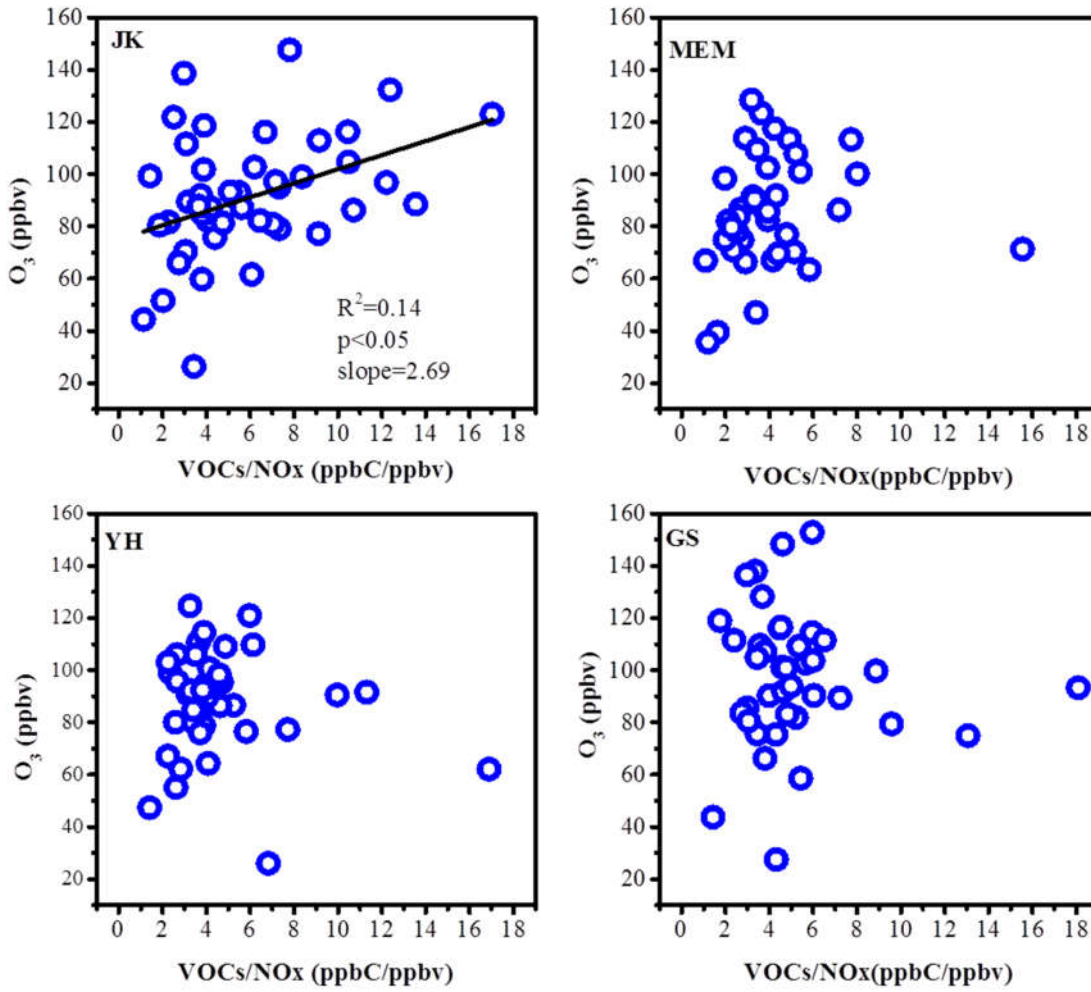
625   Fig.11 The relationship between O_3 and VOCs/NO_x at 14:00 LT

626

627

628
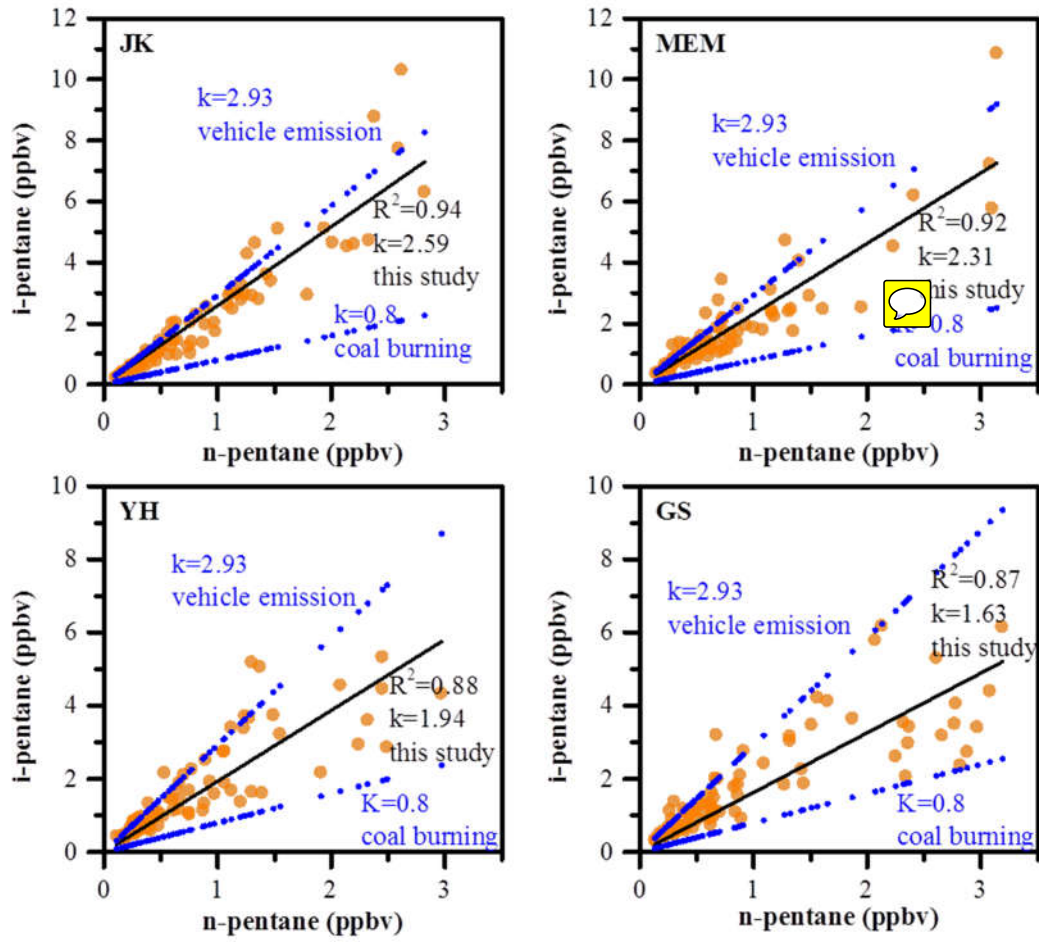
629   Fig. 12 Ratios of isopentane to n-pentane at every site

630

631
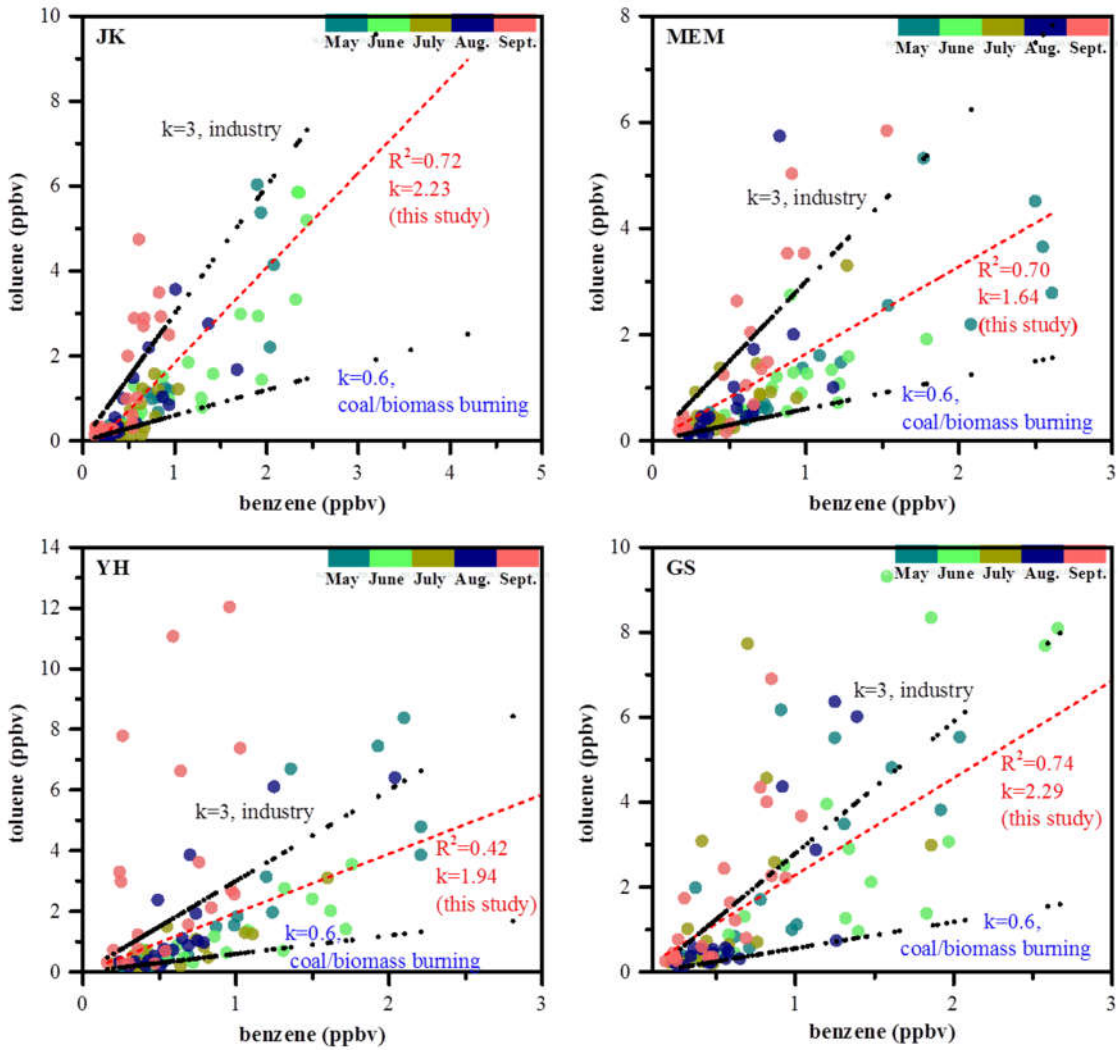
Fig.13 T/B ratios and linear correlation coefficients (R^2) between benzene and toluene at every site, the data points were color mapped with sampling period.

637
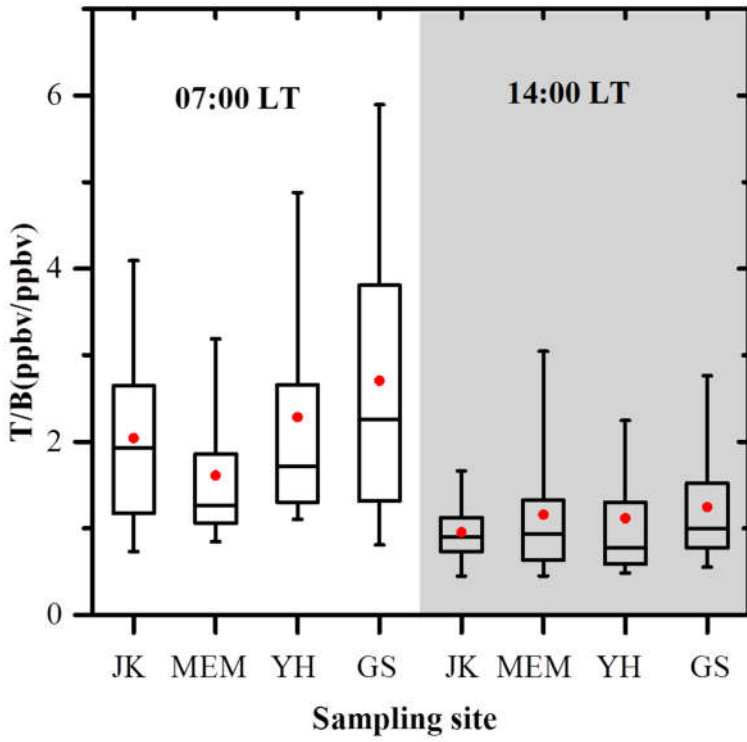
638

639   Fig. 14 The average ratio of T/B at 07:00LT and 14:00LT for each site during the whole sampling period

640

641
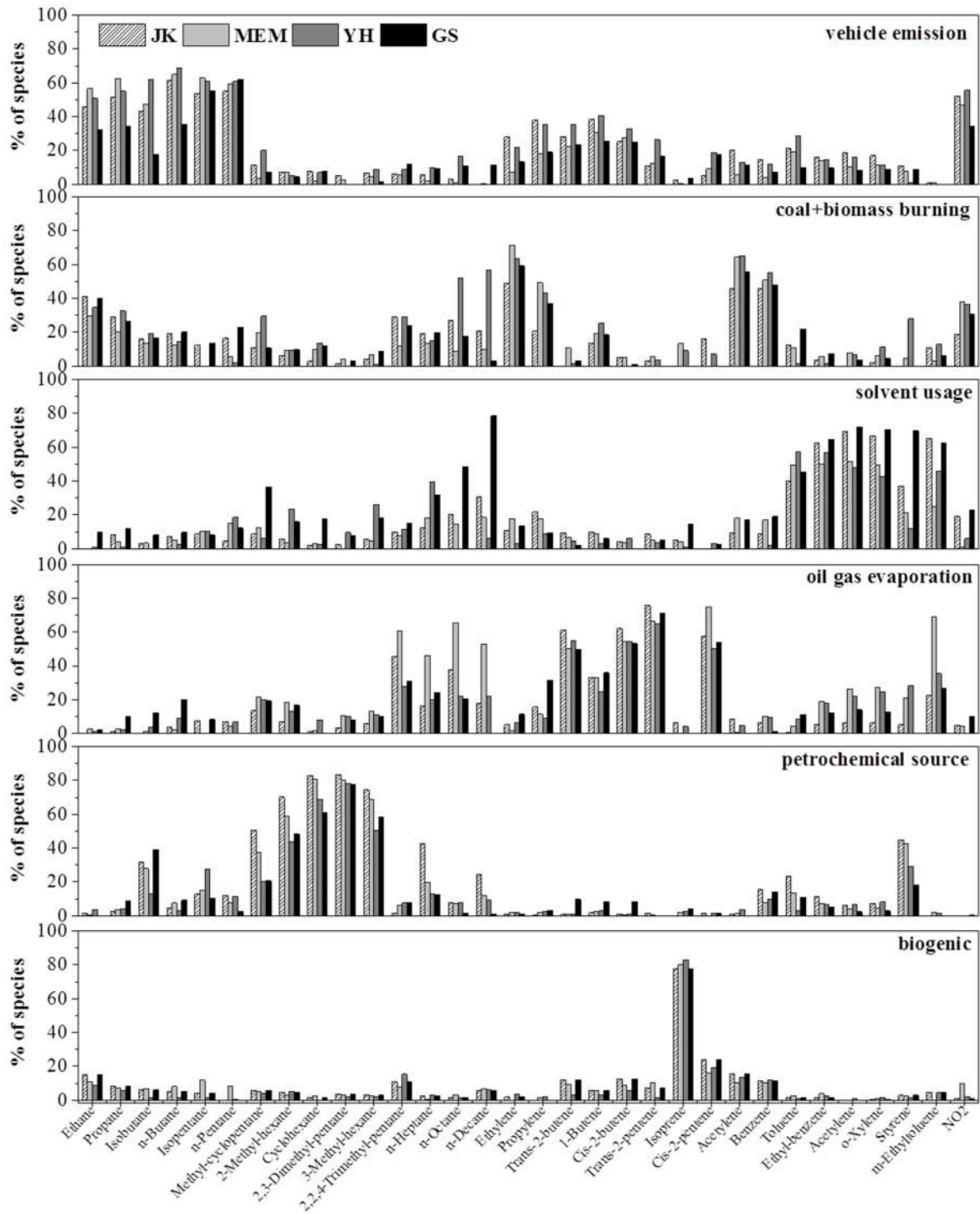
Fig. 15 Explained variations in source profiles as identified by PMF

642

643

644

645
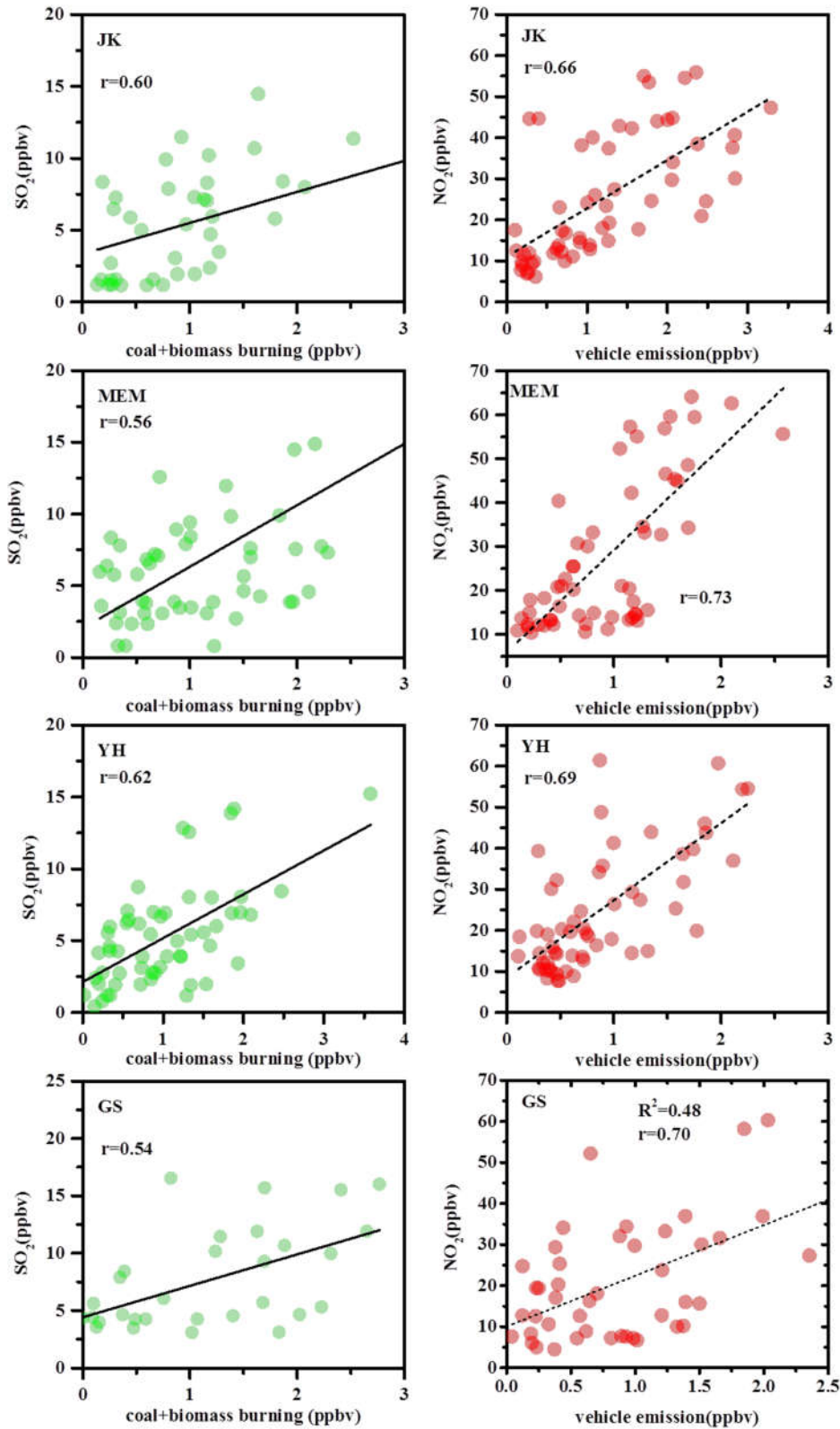
646   Fig. 16 Correlation analysis ~~between~~ contributions of coal+biomass burning and ~~SO₂, and~~ vehicle emission and

647   ~~NO₂~~

648
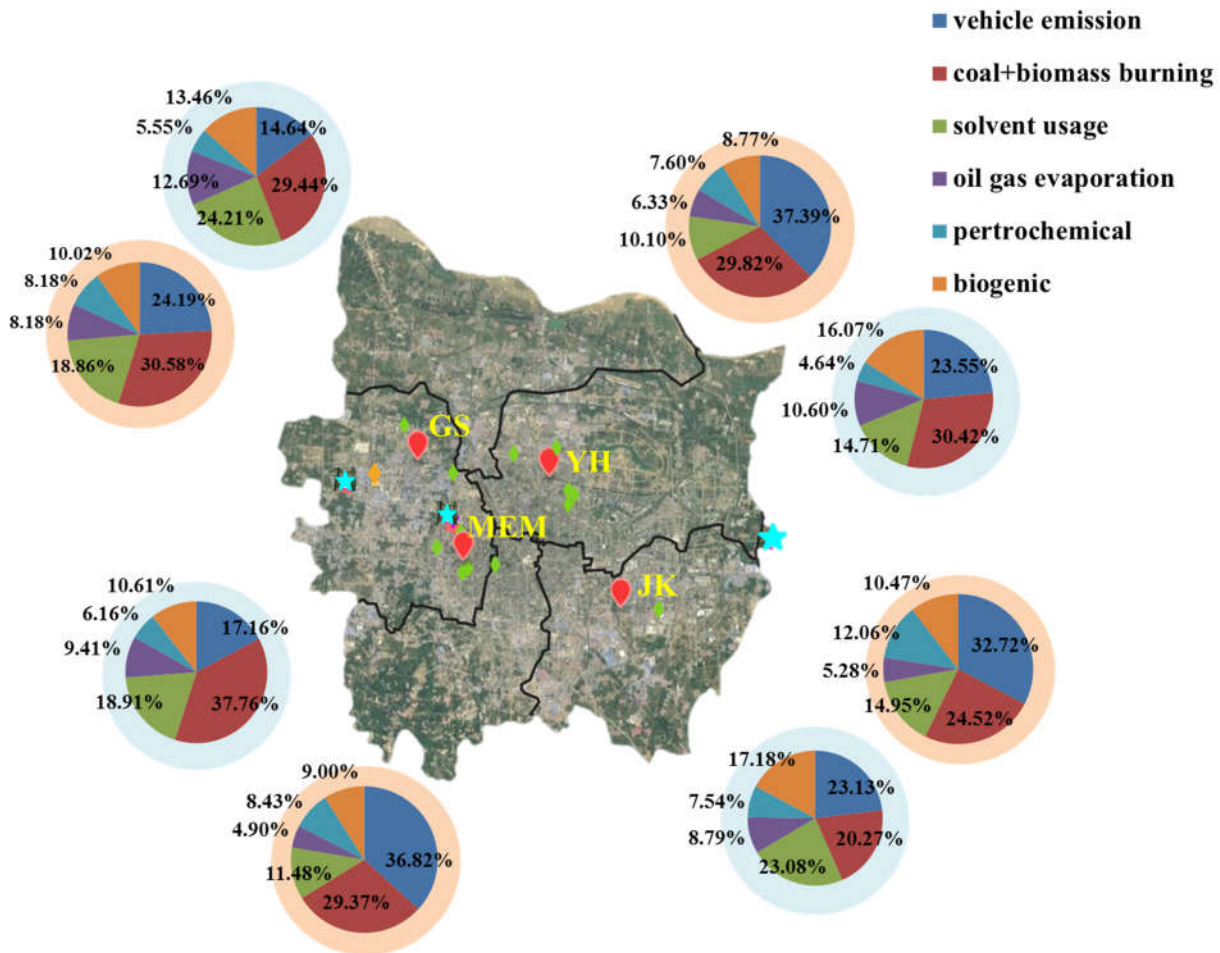
Fig. 17 Source apportionment results during the whole sampling period. The results weighted in observed concentrations were shadowed with pink color, and the results estimated based on OFP were shadowed with light blue color.

656

657
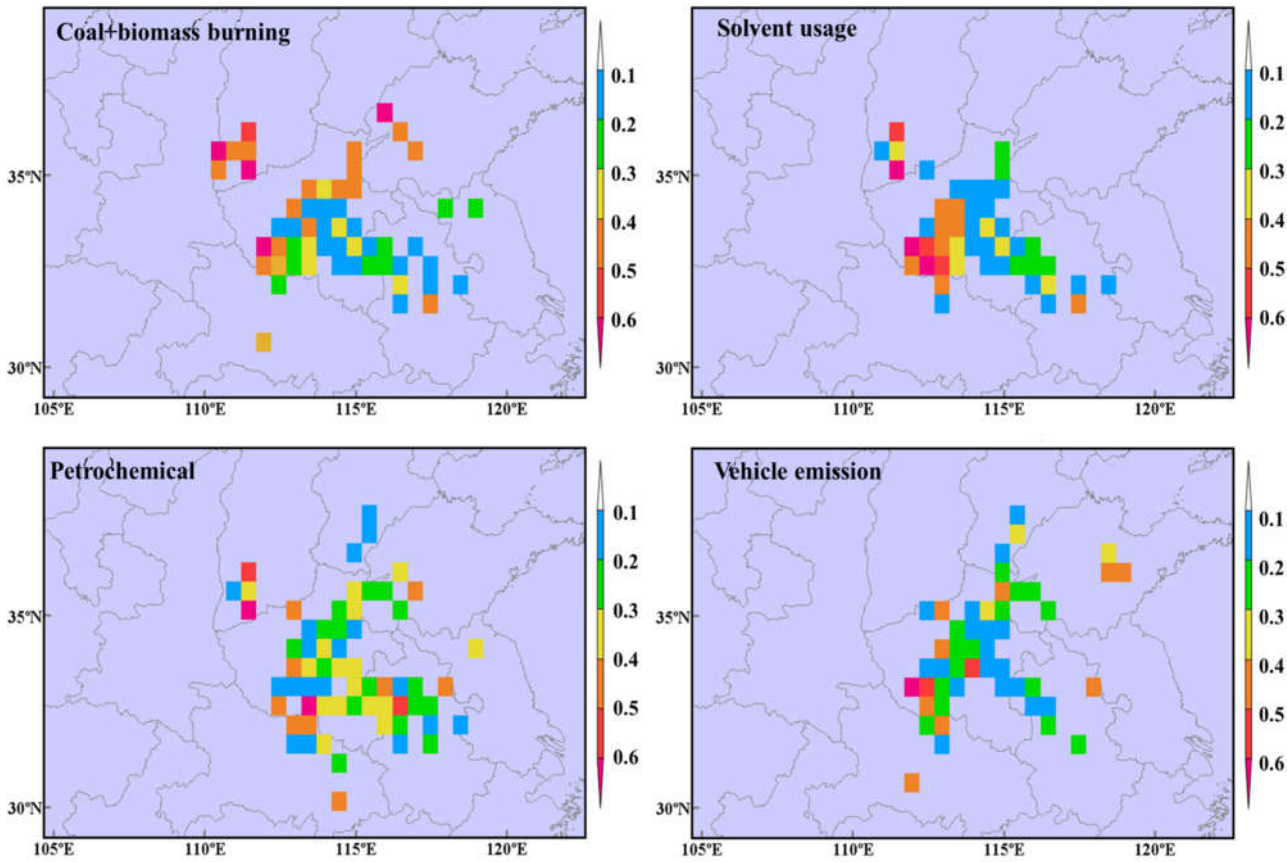
Fig. 18 Probable source regions apportioned by PSCF at Zhengzhou at summer (June-Aug. 2017) during sampling period

660

661

662
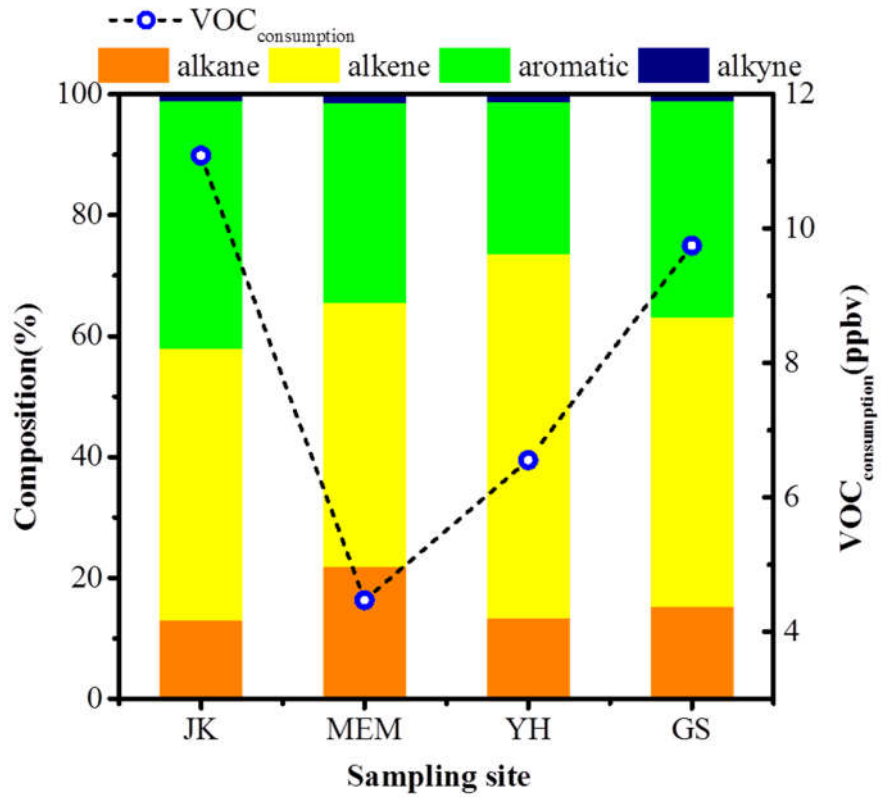
663

664   Fig. 19 The composition of major groups based on chemical consumption and the total consumption at each s

665

666 **Reference**

667 Abeleira, A., Pollack, I. B., Sive, B., Zhou, Y., Fischer, E. V., and Farmer, D. K.: Source characterization of

668 volatile organic compounds in the Colorado Northern Front Range Metropolitan Area during spring and summer

669 2015, Journal of Geophysical Research: Atmospheres, 10.1002/2016jd026227, 2017.

670 Akagi, S. K., Yokelson, R. J., Wiedinmyer, C., Alvarado, M. J., Reid, J. S., Karl, T., Crounse, J. D., and

671 Wennberg, P. O.: Emission factors for open and domestic biomass burning for use in atmospheric models,

672 Atmospheric Chemistry and Physics, 11, 4039-4072, 10.5194/acp-11-4039-2011, 2011.

673 An, J., Zhu, B., Wang, H., Li, Y., Lin, X., and Yang, H.: Characteristics and source apportionment of VOCs

674 measured in an industrial area of Nanjing, Yangtze River Delta, China, Atmospheric Environment, 97, 206-214,

675 10.1016/j.atmosenv.2014.08.021, 2014.

676 Barletta, B., Meinardi, S., Sherwood Rowland, F., Chan, C.-Y., Wang, X., Zou, S., Yin Chan, L., and Blake, D. R.:

677 Volatile organic compounds in 43 Chinese cities, Atmospheric Environment, 39, 5979-5990,

678 10.1016/j.atmosenv.2005.06.029, 2005.

679 Carter, W. P. L.: Development of Ozone Reactivity Scales for Volatile Organic Compounds, Air & Waste

680 Manage., 44, 881-899, 1994.

681 Carter, W.P.L., 2010. Development of the SAPRC-07 chemical mechanism and updated ozone reactivity scale.

682 Available at: http://www.cert.ucr.edu/ wcarter/SAPRC.

683 Chen, S.-P., Liu, T.-H., Chen, T.-F., Yang, C.-F. O., Wang, J.-L., and Chang, J. S.: Diagnostic Modeling of

684 PAMS VOC Observation, Environ. Sci. Technol., 44, 4635–4644, 2010.

685 Chen, W. T., Shao, M., Lu, S. H., Wang, M., Zeng, L. M., Yuan, B., and Liu, Y.: Understanding primary and

686 secondary sources of ambient carbonyl compounds in Beijing using the PMF model, Atmospheric Chemistry and

687 Physics, 14, 3047-3062, 10.5194/acp-14-3047-2014, 2014.

688 Cheng, L., Fu, L., Angle, R. P., and Sandhu, H. S.: Seasonal variations of volatile organic compounds in

689 Edmonton, Alberta, Atmospheric Environment, 31, 239-246, 1997.

690 Duan, J., Tan, J., Yang, L., Wu, S., and Hao, J.: Concentration, sources and ozone formation potential of volatile

691 organic compounds (VOCs) during ozone episode in Beijing, Atmospheric Research, 88, 25-35,

692 10.1016/j.atmosres.2007.09.004, 2008.

693 Gao, W., Tie, X., Xu, J., Huang, R., Mao, X., Zhou, G., and Chang, L.: Long-term trend of O3 in a mega City

694 (Shanghai), China: Characteristics, causes, and interactions with precursors, The Science of the total environment,

695 603-604, 425-433, 10.1016/j.scitotenv.2017.06.099, 2017.

696 Geng, N., Wang, J., Xu, Y., Zhang, W., Chen, C., and Zhang, R.: PM2.5 in an industrial district of Zhengzhou,

697 China: Chemical composition and source apportionment, Particuology, 11, 99-109, 10.1016/j.partic.2012.08.004,

698 2013.

699 Gentner, D. R., Worton, D. R., Isaacman, G., Davis, L. C., Dallmann, T. R., Wood, E. C., Herndon, S. C.,

700 Goldstein, A. H., and Harley, R. A.: Chemical composition of gas-phase organic carbon emissions from motor

701 vehicles and implications for ozone production, Environmental science & technology, 47, 11837-11848,

702 10.1021/es401470e, 2013.

703 Gilman, J. B., Lerner, B. M., Kuster, W. C., and de Gouw, J. A.: Source signature of volatile organic compounds

704 from oil and natural gas operations in northeastern Colorado, Environmental science & technology, 47,

705 1297-1305, 10.1021/es304119a, 2013.

Gong, M., Yin, S., Gu, X., Xu, Y., Jiang, N., and Zhang, R.: Refined 2013-based vehicle emission inventory and its spatial and temporal characteristics in Zhengzhou, China, The Science of the total environment, 599-600, 1149-1159, 10.1016/j.scitotenv.2017.03.299, 2017.

Guo, H., Cheng, H. R., Ling, Z. H., Louie, P. K., and Ayoko, G. A.: Which emission sources are responsible for the volatile organic compounds in the atmosphere of Pearl River Delta?, Journal of hazardous materials, 188, 116-124, 10.1016/j.jhazmat.2011.01.081, 2011.

Guo, H., Ling, Z. H., Cheng, H. R., Simpson, I. J., Lyu, X. P., Wang, X. M., Shao, M., Lu, H. X., Ayoko, G., Zhang, Y. L., Saunders, S. M., Lam, S. H. M., Wang, J. L., and Blake, D. R.: Tropospheric volatile organic compounds in China, The Science of the total environment, 574, 1021-1043, 10.1016/j.scitotenv.2016.09.116, 2017.

Guo, S., Tan, J., Duan, J., Ma, Y., Yang, F., He, K., and Hao, J.: Characteristics of atmospheric non-methane hydrocarbons during haze episode in Beijing, China, Environmental monitoring and assessment, 184, 7235-7246, 10.1007/s10661-011-2493-9, 2012.

Hanna, S. R., Moore, G. E., and Fernau, M.: Evaluation of photochemical grid models (UAM-IV, UAM-V, and the ROM/UAM-IV couple) using data from the Lake Michigan Ozone Study (LMOS) Atmospheric Environment 30, 3265-3279, 1996.

Hidy, G. M., and Blanchard, C. L.: Precursor reductions and ground-level ozone in the Continental United States, Journal of the Air & Waste Management Association, 65, 1261-1282, 10.1080/10962247.2015.1079564, 2015.

Ho, K. F., Lee, S. C., Ho, W. K., Blake, D. R., Cheng, Y., Li, Y. S., Ho, S. S. H., Fung, K., Louie, P. K. K., and Park, D.: Vehicular emission of volatile organic compounds (VOCs) from a tunnel study in Hong Kong, Atmos. Chem. Phys., 9, 7491–7504, 2009.

Hopke, P. K., Barrie, L. A., Li, S.-M., M.-D.Cheng, C.Li, and Xie, Y.: Possible sources and preferred pathways for biogenic and non-sea-salt sulfur for the high Arctic Journal of Geophysical Research, 100, 16,595-516,603, 1995.

Huang, X., Zhang, Y., Yang, W., Huang, Z., Wang, Y., Zhang, Z., He, Q., Lü, S., Huang, Z., Bi, X., and Wang, X.: Effect of traffic restriction on reducing ambient volatile organic compounds (VOCs): Observation-based evaluation during a traffic restriction drill in Guangzhou, China, Atmospheric Environment, 161, 61-70, 10.1016/j.atmosenv.2017.04.035, 2017.

Huang, Y., Ling, Z. H., Lee, S. C., Ho, S. S. H., Cao, J. J., Blake, D. R., Cheng, Y., Lai, S. C., Ho, K. F., Gao, Y., Cui, L., and Louie, P. K. K.: Characterization of volatile organic compounds at a roadside environment in Hong Kong: An investigation of influences after air pollution control strategies, Atmospheric Environment, 122, 809-818, 10.1016/j.atmosenv.2015.09.036, 2015.

Jia, C., Mao, X., Huang, T., Liang, X., Wang, Y., Shen, Y., Jiang, W., Wang, H., Bai, Z., Ma, M., Yu, Z., Ma, J., and Gao, H.: Non-methane hydrocarbons (NMHCs) and their contribution to ozone formation potential in a petrochemical industrialized city, Northwest China, Atmospheric Research, 169, 225-236, 10.1016/j.atmosres.2015.10.006, 2016.

Jiang, X., Guenther, A., Potosnak, M., Geron, C., Seco, R., Karl, T., Kim, S., Gu, L., and Pallardy, S.: Isoprene emission response to drought and the impact on global atmospheric chemistry, Atmospheric Environment, 183, 69-83, 10.1016/j.atmosenv.2018.01.026, 2018.

Jin, X., and Holloway, T.: Spatial and temporal variability of ozone sensitivity over China observed from the Ozone Monitoring Instrument, Journal of Geophysical Research: Atmospheres, 120, 7229-7246, 10.1002/2015jd023250, 2015.

Jobson, B. T., Berkowitz, C. M., Kuster, W. C., Goldan, P. D., Williams, E. J., Fesenfeld, F. C., Apel, E. C., Karl, T., Lonneman, W. A., and Riemer, D.: Hydrocarbon source signatures in Houston, Texas: Influence of the petrochemical industry, Journal of Geophysical Research, 109, 10.1029/2004jd004887, 2004.

Lau, A. K., Yuan, Z., Yu, J. Z., and Louie, P. K.: Source apportionment of ambient volatile organic compounds in Hong Kong, The Science of the total environment, 408, 4138-4149, 10.1016/j.scitotenv.2010.05.025, 2010.

Li, B., Ho, S. S. H., Xue, Y., Huang, Y., Wang, L., Cheng, Y., Dai, W., Zhong, H., Cao, J., and Lee, S.: Characterizations of volatile organic compounds (VOCs) from vehicular emissions at roadside environment: The first comprehensive study in Northwestern China, Atmospheric Environment, 161, 1-12, 10.1016/j.atmosenv.2017.04.029, 2017a.

Li, K., Chen, L., Ying, F., White, S. J., Jang, C., Wu, X., Gao, X., Hong, S., Shen, J., Azzi, M., and Cen, K.: Meteorological and chemical impacts on ozone formation: A case study in Hangzhou, China, Atmospheric Research, 10.1016/j.atmosres.2017.06.003, 2017b.

Li, L., and Wang, X.: Seasonal and diurnal variations of atmospheric non-methane hydrocarbons in Guangzhou, China, International journal of environmental research and public health, 9, 1859-1873, 10.3390/ijerph9051859, 2012.

Li, L., Chen, Y., Zeng, L., Shao, M., Xie, S., Chen, W., Lu, S., Wu, Y., and Cao, W.: Biomass burning contribution to ambient volatile organic compounds (VOCs) in the Chengdu–Chongqing Region (CCR), China, Atmospheric Environment, 99, 403-410, 10.1016/j.atmosenv.2014.09.067, 2014.

Li, Q., Zhang, L., Wang, T., Wang, Z., Fu, X., and Zhang, Q.: "New" Reactive Nitrogen Chemistry Reshapes the Relationship of Ozone to Its Precursors, Environmental science & technology, 52, 2810-2818, 10.1021/acs.est.7b05771, 2018.

Lin, X., Traner, M., and Liu, S. C.: On the Nonlinearity of the Tropospheric Ozone Production, Journal Of Geophysical Research, 93, 15879-15888, 1998.

Liu, B., Liang, D., Yang, J., Dai, Q., Bi, X., Feng, Y., Yuan, J., Xiao, Z., Zhang, Y., and Xu, H.: Characterization and source apportionment of volatile organic compounds based on 1-year of observational data in Tianjin, China, Environmental pollution, 218, 757-769, 10.1016/j.envpol.2016.07.072, 2016.

Liu, C., Ma, Z., Mu, Y., Liu, J., Zhang, C., Zhang, Y., Liu, P., and Zhang, H.: The levels, variation characteristics, and sources of atmospheric non-methane hydrocarbon compounds during wintertime in Beijing, China, Atmospheric Chemistry and Physics, 17, 10633-10649, 10.5194/acp-17-10633-2017, 2017.

Liu, Y., Shao, M., Fu, L., Lu, S., Zeng, L., and Tang, D.: Source profiles of volatile organic compounds (VOCs) measured in China: Part I, Atmospheric Environment, 42, 6247-6260, 10.1016/j.atmosenv.2008.01.070, 2008.

Liu, Y., Yuan, B., Li, X., Shao, M., Lu, S., Li, Y., Chang, C. C., Wang, Z., Hu, W., Huang, X., He, L., Zeng, L., Hu, M., and Zhu, T.: Impact of pollution controls in Beijing on atmospheric oxygenated volatile organic compounds (OVOCs) during the 2008 Olympic Games: observation and modeling implications, Atmospheric Chemistry and Physics, 15, 3045-3062, 10.5194/acp-15-3045-2015, 2015.

Louie, P. K. K., Ho, J. W. K., Tsang, R. C. W., Blake, D. R., Lau, A. K. H., Yu, J. Z., Yuan, Z., Wang, X., Shao, M., and Zhong, L.: VOCs and OVOCs distribution and control policy implications in Pearl River Delta region, China, Atmospheric Environment, 76, 125-135, 10.1016/j.atmosenv.2012.08.058, 2013.

Luecken, D. J., Napelenok, S. L., Strum, M., Scheffe, R., and Phillips, S.: Sensitivity of Ambient Atmospheric Formaldehyde and Ozone to Precursor Species and Source Types Across the United States, Environmental science & technology, 52, 4668-4675, 10.1021/acs.est.7b05509, 2018.

Lyu, X. P., Chen, N., Guo, H., Zhang, W. H., Wang, N., Wang, Y., and Liu, M.: Ambient volatile organic compounds and their effect on ozone production in Wuhan, central China, The Science of the total environment, 541, 200-209, 10.1016/j.scitotenv.2015.09.093, 2016.

Malley, C. S., Braban, C. F., Dumitrean, P., Cape, J. N., and Heal, M. R.: The impact of speciated VOCs on regional ozone increment derived from measurements at the UK EMEP supersites between 1999 and 2012, Atmospheric Chemistry and Physics, 15, 8361-8380, 10.5194/acp-15-8361-2015, 2015.

McGaughey, G. R., Desai, N. R., Allen, D. T., Seila, R. L., Lonneman, W. A., Fraser, M. P., Harley, R. A., Pollack, A. K., Ivy, J. M., and Price, J. H.: Analysis of motor vehicle emissions in a Houston tunnel during the Texas Air Quality Study 2000, Atmospheric Environment, 38, 3363-3372, 10.1016/j.atmosenv.2004.03.006, 2004.

Mu, B., Mayer, A. L., He, R., and Tian, G.: Land use dynamics and policy implications in Central China: A case study of Zhengzhou, Cities, 58, 39-49, 10.1016/j.cities.2016.05.012, 2016.

Na, K., Kim, Y. P., Moon, K.-C., Moon, I., and Fung, K.: Concentrations of volatile organic compounds in an industrial area of Korea, Atmospheric Environment 35, 2747-2756, 2001.

Nagashima, T., Sudo, K., Akimoto, H., Kurokawa, J., and Ohara, T.: Long-term change in the source contribution to surface ozone over Japan, Atmospheric Chemistry and Physics, 17, 8231-8246, 10.5194/acp-17-8231-2017, 2017.

Ou, J., Zheng, J., Li, R., Huang, X., Zhong, Z., Zhong, L., and Lin, H.: Speciated OVOC and VOC emission inventories and their implications for reactivity-based ozone control strategy in the Pearl River Delta region, China, The Science of the total environment, 530-531, 393-402, 10.1016/j.scitotenv.2015.05.062, 2015.

Ou, J., Yuan, Z., Zheng, J., Huang, Z., Shao, M., Li, Z., Huang, X., Guo, H., and Louie, P. K.: Ambient Ozone Control in a Photochemically Active Region: Short-Term Despiking or Long-Term Attainment?, Environmental science & technology, 50, 5720-5728, 10.1021/acs.est.6b00345, 2016.

Pal, S., Xueref-Remy, I., Ammoura, L., Chazette, P., Gibert, F., Royer, P., Dieudonné, E., Dupont, J. C., Haeffelin, M., Lac, C., Lopez, M., Morille, Y., and Ravetta, F.: Spatio-temporal variability of the atmospheric boundary layer depth over the Paris agglomeration: An assessment of the impact of the urban heat island intensity, Atmospheric Environment, 63, 261-275, 10.1016/j.atmosenv.2012.09.046, 2012.

Polissar, A. V., Hopke, P. K., Paatero, P., Kaufmann, Y. J., Hall, D. K., Bodhaine, B. A., Dutton, E. G., and Harris, J. M.: The aerosol at Barrow, Alaska: long-term trends and source locations, Atmospheric Environment 33, 2441-2458, 1999.

Pollack, I. B., Ryerson, T. B., Trainer, M., Neuman, J. A., Roberts, J. M., and Parrish, D. D.: Trends in ozone, its precursors, and related secondary oxidation products in Los Angeles, California: A synthesis of measurements from 1960 to 2010, Journal of Geophysical Research: Atmospheres, 118, 5893-5911, 10.1002/jgrd.50472, 2013.

Raysoni, A. U., Stock, T. H., Sarnat, J. A., Chavez, M. C., Sarnat, S. E., Montoya, T., Holguin, F., and Li, W. W.: Evaluation of VOC concentrations in indoor and outdoor microenvironments at near-road schools, Environmental pollution, 231, 681-693, 10.1016/j.envpol.2017.08.065, 2017.

Russo, R. S., Zhou, Y., White, M. L., Mao, H., Talbot, R., and Sive, B. C.: Multi-year (2004–2008) record of nonmethane hydrocarbons and halocarbons in New England: seasonal variations and regional sources, Atmospheric Chemistry and Physics, 10, 4909-4929, 10.5194/acp-10-4909-2010, 2010.

Sahu, L. K., Tripathi, N., and Yadav, R.: Contribution of biogenic and photochemical sources to ambient VOCs during winter to summer transition at a semi-arid urban site in India, Environmental pollution, 229, 595-606, 10.1016/j.envpol.2017.06.091, 2017.

831 Shao, M., Lu, S., Liu, Y., Xie, X., Chang, C., Huang, S., and Chen, Z.: Volatile organic compounds measured in
832 summer in Beijing and their role in ground-level ozone formation, Journal of Geophysical Research, 114,
833 10.1029/2008jd010863, 2009.

834 Shao, M., Wang, B., Lu, S., Yuan, B., and Wang, M.: Effects of Beijing Olympics Control Measures on Reducing
835 Reactive Hydrocarbon Species, Environ. Sci. Technol., 45, 514-519, 2011.

836 Shao, P., An, J., Xin, J., Wu, F., Wang, J., Ji, D., and Wang, Y.: Source apportionment of VOCs and the
837 contribution to photochemical ozone formation during summer in the typical industrial area in the Yangtze River
838 Delta, China, Atmospheric Research, 176-177, 64-74, 10.1016/j.atmosres.2016.02.015, 2016.

839 Shen, F., Ge, X., Hu, J., Nie, D., Tian, L., and Chen, M.: Air pollution characteristics and health risks in Henan
840 Province, China, Environmental research, 156, 625-634, 10.1016/j.envres.2017.04.026, 2017.

841 Shiu, C.-J., Liu, S. C., Chang, C.-C., Chen, J.-P., Chou, C. C. K., Lin, C.-Y., and Young, C.-Y.: Photochemical
842 production of ozone and control strategy for Southern Taiwan, Atmospheric Environment, 41, 9324-9340,
843 10.1016/j.atmosenv.2007.09.014, 2007.

844 Sillman, S.: The relation between ozone, NOx and hydrocarbons in urban and polluted rural environments,
845 Atmospheric Environment 33, 1821-1845, 1999.

846 Streets, D. G., Fu, J. S., Jang, C. J., Hao, J., He, K., Tang, X., Zhang, Y., Wang, Z., Li, Z., Zhang, Q., Wang, L.,
847 Wang, B., and Yu, C.: Air quality during the 2008 Beijing Olympic Games, Atmospheric Environment, 41,
848 480-492, 10.1016/j.atmosenv.2006.08.046, 2007.

849 Sun, J., Wu, F., Hu, B., Tang, G., Zhang, J., and Wang, Y.: VOC characteristics, emissions and contributions to
850 SOA formation during hazy episodes, Atmospheric Environment, 141, 560-570, 10.1016/j.atmosenv.2016.06.060,
851 2016.

852 Tang, J. H., Chan, L. Y., Chan, C. Y., Li, Y. S., Chang, C. C., Liu, S. C., Wu, D., and Li, Y. D.: Characteristics
853 and diurnal variations of NMHCs at urban, suburban, and rural sites in the Pearl River Delta and a remote site in
854 South China, Atmospheric Environment, 41, 8620-8632, 10.1016/j.atmosenv.2007.07.029, 2007.

855 Tsai, S. M., Zhang, J. J., Smith, K. R., Ma, Y., Rasmussen, R. A., and Khalil, M. A. K.: Characterization of
856 Non-methane Hydrocarbons Emitted from Various Cookstoves Used in China, Environ. Sci. Technol., 37,
857 2869-2877, 2003.

858 Wang, H.-l., Jing, S.-a., Lou, S.-r., Hu, Q.-y., Li, L., Tao, S.-k., Huang, C., Qiao, L.-p., and Chen, C.-h.: Volatile
859 organic compounds (VOCs) source profiles of on-road vehicle emissions in China, The Science of the total
860 environment, 607-608, 253-261, 10.1016/j.scitotenv.2017.07.001, 2017a.

861 Wang, H., Qiao, Y., Chen, C., Lu, J., Qiao, L., and Lou, S.: Source Profiles and Chemical Reactivity of Volatile
862 Organic Compounds from Solvent Use in Shanghai, China, Aerosol and Air Quality Research,
863 10.4209/aaqr.2013.03.0064, 2014.

864 Wang, M., Shao, M., Lu, S.-H., Yang, Y.-D., and Chen, W.-T.: Evidence of coal combustion contribution to
865 ambient VOCs during winter in Beijing, Chinese Chemical Letters, 24, 829-832, 10.1016/j.cclet.2013.05.029,
866 2013.

867 Wang, M., Shao, M., Chen, W., Lu, S., Liu, Y., Yuan, B., Zhang, Q., Zhang, Q., Chang, C. C., Wang, B., Zeng,
868 L., Hu, M., Yang, Y., and Li, Y.: Trends of non-methane hydrocarbons (NMHC) emissions in Beijing during
869 2002–2013, Atmospheric Chemistry and Physics, 15, 1489-1502, 10.5194/acp-15-1489-2015, 2015.

870 Wang, T., Xue, L., Brimblecombe, P., Lam, Y. F., Li, L., and Zhang, L.: Ozone pollution in China: A review of
871 concentrations, meteorological influences, chemical precursors, and effects, The Science of the total environment,
872 575, 1582-1596, 10.1016/j.scitotenv.2016.10.081, 2017b.

Wang, X.-m., Sheng, G.-y., Fu, J.-m., Chan, C.-y., Lee, S.-C., Chan, L. Y., and Wang, Z.-s.: Urban roadside aromatic hydrocarbons in three cities of the Pearl River Delta, People's Republic of China, Atmospheric Environment, 36, 5141–5148, 2002.

Wei, W., Cheng, S., Li, G., Wang, G., and Wang, H.: Characteristics of ozone and ozone precursors (VOCs and NOx) around a petroleum refinery in Beijing, China, Journal of Environmental Sciences, 26, 332-342, 10.1016/s1001-0742(13)60412-x, 2014.

Wu, R., and Xie, S.: Spatial Distribution of Ozone Formation in China Derived from Emissions of Speciated Volatile Organic Compounds, Environmental science & technology, 51, 2574-2583, 10.1021/acs.est.6b03634, 2017.

Xue, Y., Ho, S. S. H., Huang, Y., Li, B., Wang, L., Dai, W., Cao, J., and Lee, S.: Source apportionment of VOCs and their impacts on surface ozone in an industry city of Baoji, Northwestern China, Scientific Reports, 7, 9979, 10.1038/s41598-017-10631-4, 2017.

Yan, Y., Peng, L., Li, R., Li, Y., Li, L., and Bai, H.: Concentration, ozone formation potential and source analysis of volatile organic compounds (VOCs) in a thermal power station centralized area: A study in Shuozhou, China, Environmental pollution, 223, 295-304, 10.1016/j.envpol.2017.01.026, 2017.

Yuan, B., Shao, M., de Gouw, J., Parrish, D. D., Lu, S., Wang, M., Zeng, L., Zhang, Q., Song, Y., Zhang, J., and Hu, M.: Volatile organic compounds (VOCs) in urban air: How chemistry affects the interpretation of positive matrix factorization (PMF) analysis, Journal of Geophysical Research: Atmospheres, 117, n/a-n/a, 10.1029/2012jd018236, 2012.

Zhang, J., Sun, Y., Wu, F., Sun, J., and Wang, Y.: The characteristics, seasonal variation and source apportionment of VOCs at Gongga Mountain, China, Atmospheric Environment, 88, 297-305, 10.1016/j.atmosenv.2013.03.036, 2014.

Zhang, Z., Wang, X., Zhang, Y., Lu, S., Huang, Z., Huang, X., and Wang, Y.: Ambient air benzene at background sites in China's most developed coastal regions: exposure levels, source implications and health risks, The Science of the total environment, 511, 792-800, 10.1016/j.scitotenv.2015.01.003, 2015.

Zhu, Y., Yang, L., Chen, J., Wang, X., Xue, L., Sui, X., Wen, L., Xu, C., Yao, L., Zhang, J., Shao, M., Lu, S., and Wang, W.: Characteristics of ambient volatile organic compounds and the influence of biomass burning at a rural site in Northern China during summer 2013, Atmospheric Environment, 124, 156-165, 10.1016/j.atmosenv.2015.08.097, 2016.